AN ABSTRACT OF THE THESIS OF

Matthew G. Peterson for the degree of Master of Science in Wood Science presented on December 15, 2009.
Title: The Potential of Using Log Biometrics to Track Sawmill Flow

Abstract approved:

_____

Charles C. Brunner

We studied the feasibility of using end-grain characteristics to match individual boards and cants back to their parent Douglas-fir (*Pseudotsuga menziesii*) logs. After reviewing marking/reading and biometric automated identification systems, we focused on end-grain biometrics because they appear to have the most promise for sawmills. Biometric identification requires that every individual be unique in some quantifiable way and that the trait used remain relatively unchanged over time. To determine whether end-grain characteristics could meet these requirements, we imaged 120 Douglas-fir cross-sections three times over the span of three days. An image matching algorithm matched images cropped to simulate cants and boards to cross-section images taken at an earlier time. We analyzed the results using standard receiver operating characteristic curves commonly used to evaluate biometric identification systems. Results showed that 98% of the day 2 board images were correctly matched back to their day 1 parent cant images, and 93% for the day 3 to the day 2 images. When cants were matched to uncropped rounds, 88% of the day 2 images were correctly matched to the day 1 images, and 83% for the day 3 to day 2

images. The results are encouraging because they suggest that individual logs can be identified using the variability of end-grain characteristics.

The Potential of Using Log Biometrics to Track Sawmill Flow

by
Matthew G. Peterson

A THESIS

submitted to

Oregon State University

in partial fulfillment of
the requirements for the
degree of

Master of Science

Presented December 15, 2009
Commencement June 2010

Master of Science thesis of Matthew G. Peterson presented on December 15, 2009.

APPROVED:

Major Professor, representing Wood Science

Head of the Department of Wood Science and Engineering

Dean of the Graduate School

I understand that my thesis will become part of the permanent collection of Oregon State University libraries. My signature below authorizes release of my thesis to any reader upon request.

Matthew G. Peterson, Author

ACKNOWLEDGEMENTS

I would like to extend my sincere appreciation to my major professor, Dr. Charles Brunner, for his invaluable support, assistance, and guidance throughout my Master's program and beyond. I would also like to convey my sincere gratitude to Dr. James Reeb and Dr. David Porter for providing their expert advice and knowledge of identification systems and material tracking concepts.

Special thanks go to Adin Berberovic, who allowed us to use his software for our analysis. I would also like to give special thanks to Jeff Vaughn, who generously gave his time and his chainsaw experience to help make our project a reality, as well as Dr. Jeffrey Morrell, who donated his material for our project.

In addition, I would like to thank the faculty, staff, and students in the Wood Science and Engineering Department and in the Mechanical, Industrial, and Manufacturing Engineering Department who have made my experience at OSU fruitful, challenging, and unforgettable.

I extend my gratitude to my family for their love and support they have given me throughout my life, and making me the person I am today. Finally, I save my last words for my wife, Janice, for everything that we share, for her love, and for her support of my dreams and goals; thank you.

TABLE OF CONTENTS

Page

LIST OF FIGURES

LIST OF FIGURES (Continued)

Figure Page

LIST OF TABLES

The Potential of Using Log Biometrics to Track Sawmill Flow

1. INTRODUCTION

In an increasingly competitive global market, U.S. sawmills are challenged with becoming more efficient while improving quality (Wagner et al. 1998). Consequently, sawmill managers increasingly use quality improvement principles to maximize lumber recovery and value (Young and Winistorfer 1999). Successful applications of these principles require detailed information of every manufacturing step (Wall 1995).

Many advances in the automated detection of wood characteristics are used to optimize processing and increase lumber recovery. However, research into the use of material flow research for sawmills is in its infancy (Maness 1993; Funck et al. 2000). According to Wall (1995), monitoring material flow through the production process can drastically improve product quality and increase production efficiency by up to 80 percent. While the advantages of automatically tracking material flow is well understood and commonplace in many industries, it has not yet been successfully implemented in a sawmilling environment.

There are several technologies available to track material flow. The most common, and well-known, technologies are radio-frequency and barcode identification, also known as marking/reading systems (Chiorescu et al. 2003). Both systems require an identification tag be placed on each individual -- a process that is too costly and complex for a typical sawmill.

Another tracking technology explored for use in the forest products industry is biometric identification, also known as marking/reading-free systems (Chiorescu et al. 2003). Systems based on this technology rely on identifying individual cants and boards back to their parent logs using their physiological *characteristics*, which are physiological aspects of an individual that can be measured quantitatively (Chiorescu et al. 2003; Luis-Garcia et al. 2003; Jain et al. 2004).

For the purposes of this study, a cant will be defined as the breakdown component of a log that is reduced to a rectangular in cross section after processing by the headrig, or primary breakdown saw. Boards are defined as the breakdown components of a cant that are reduced to standard 2-by lumber sizes after processing by the gangsaw. An example of a log, cant, and boards are seen in Figure 1. Implementing biometric identification in a sawmill is challenging because as logs are processed into boards the original characteristic may be altered or even entirely removed.

Research utilizing log biometrics has focused on longitudinal characteristics such as geometric shape to identify logs and face-grain patterns to identify boards. These techniques rely on characteristics that are altered as the log is processed, which makes them unreliable comprehensive material tracking between machine centers. Evaluation of these techniques has also lacked methodological consistency making it difficult to compare them.

Our research is focused on end-grain, which is located on a log's cross-section and consists mainly of the annual rings of concentric latewood and earlywood bands

(Figure 1). As logs are processed, the end-grain surface is theoretically untouched until the very end of the process. No previous studies have used the variability of end-grain characteristics to identify "children" boards back to their "parent" logs.

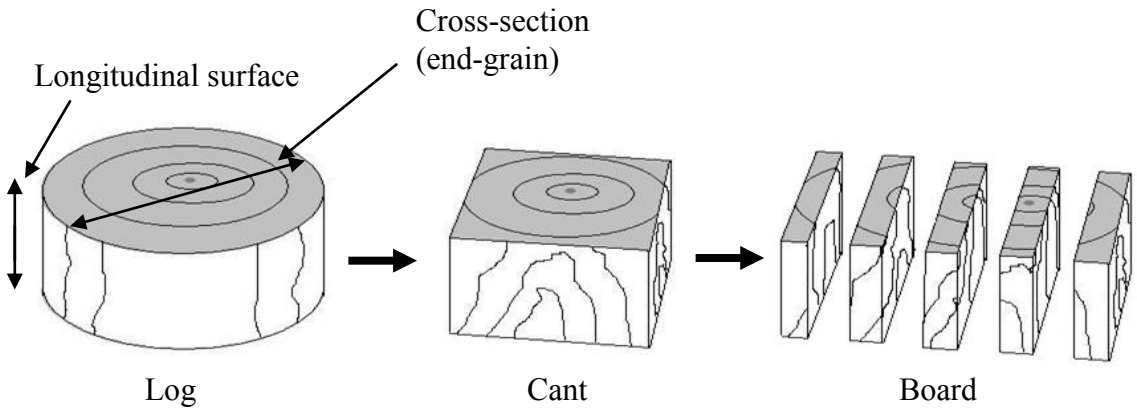

Figure 1. Drawing of a log, cant, and boards showing the longitudinal and cross-sectional dimensions.

1.1. Objective

The objective of this study is to determine whether there is sufficient variability in Douglas-fir end-grain to uniquely identify cants and boards back to their parent logs. A secondary, but important, objective is to apply standard biometric identification analysis procedures to measure this technique's effectiveness.

1.2. Hypotheses

- Douglas-fir end-grain possesses sufficient variability to match sawn boards back to their respective cant end-grain.

- Douglas-fir end-grain possesses sufficient variability to match sawn cants back to their respective rounds, or log, end-grain.

2. LITERATURE REVIEW

In this section, we will discuss the meaning of material tracking, also known as traceability, and its benefits for sawmills. We will review two types of material tracking systems: marking/reading systems, which include radio-frequency and barcode identification; and biometric identification systems, which will be our primary focus. An argument will then be presented for identifying logs, cants, and boards using end-grain characteristics.

2.1. Definition of traceability

Traceability can be defined as attaching a unique identifier to a product to collect and monitor production and distribution history (Maness 1993; Wall 1995). Many industries rely on traceability to track raw materials and products throughout their supply chains. The food industry must maintain accurate and timely records of food from production to the consumer to quickly quarantine or recall contaminated products.

To track material through a sawmill, an automated system would need to identify individual logs, cants, and boards (Maness 1993; Wall 1995), and maintain a record of their parent-child relationship as they are processed through machine centers. Tracking systems are thus designed to connect every processing step by collecting, analyzing, and distributing production data in real-time, which can drastically improve quality and efficiency (Wall 1995). Figure 2 shows how extensively material and information flow could be monitored and disseminated

through a sawmill as at every machine center each workpiece could be traced to its parent log. This information would be transmitted to a host computer that monitors the entire production process providing an increased understanding, of machine center interactions.

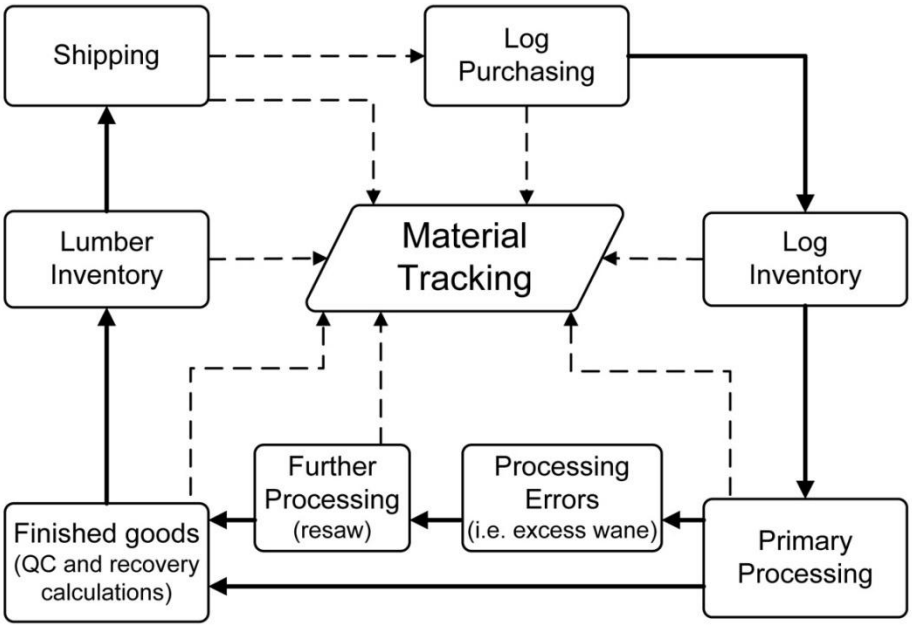

Figure 2. An adaptation of the Stevens Advanced Weighing Systems Ltd. approach to materials traceability showing how material flow could be monitored in a sawmill (Wall 1995). Solid lines represent material flow, and dotted lines represent identification information flow.

2.2. Benefits of sawmill material tracking systems

Material tracking systems are not used in the forest products industry because they are difficult to implement, not well understood, and difficult to maintain (Chiorescu et al. 2003). Despite the difficulties of implementing tracking systems, they can improve manufacturing systems by providing accurate data for making more

informed production decisions. They also have implications for reducing environmental impacts by creating a framework for chain-of-custody documentation required for environmental certification.

2.2.1. System benefit

A typical sawmill contains a complex array of machine centers that automatically execute programmed cutting solutions quickly and accurately. However, each machine center works individually, regardless of the optimization decisions made up- and down-stream. The board edger that relies on its own sensor data and optimization program can modify an optimized log cutting solution made at the headrig. This lack of integration can lead to inefficient processing and a general lack of clarity for the entire system (Maness 1993; Wall 1995).

Maness (1993) described how an identification system could increase information flow between machine centers by tracking parent-child relationships through the log breakdown process and thus provide real-time monitoring of piece flow. He proposes that a tracking system could connect optimizer scanning data to the parent logs providing the ability to optimize the entire sawmill system, which is difficult to do manually, and is virtually never performed (Maness 1993).

Maness (1993) evaluated this concept using twenty-nine logs scanned with a log scanner employing value-based sawing optimization. The log scanner used laser triangulation to capture the log's exterior shape, which was then used to calculate its optimal cutting pattern based on volume and value. The cants processed at the headrig

were labeled with the log's identification number as well as its location in the headrig scanner's sawing solution before being sawn on an optimizing gangsaw. The predicted volume and value were then compared to the actual output. The final board dimensions were also compared to the headrig optimizer's sawing solution.

Maness (1993) found that the volumes and values calculated for the 29 sawlogs by the headrig optimizer were lower than the actual output with a predicted volume of 790 board-feet (BF) from 76 boards compared to an actual volume of 656 BF from only 75 boards. The difference arose from more 1x4 material being produced instead of the 2x4 material predicted by the log optimizer resulting in an actual product value 20% less than was predicted.

Maness identified three possible causes of these discrepancies: inaccurate log scanning, poor equipment setup, or inconsistent price tables used at one or more machine centers. These issues are difficult to diagnose, because final value is not determined until the lumber is graded after processing when all log to lumber relationships are lost. Sirkka (2008) agrees, stating that dimensional lumber is considered a bulk material, and is graded after processing to determine if customer demands are met. Quality control is performed manually on a small subset of boards, which finds processing errors without revealing their cause or location (Maness 1993; Wall 1995).

The disparity between actual and predicted value and volume has implications for production planning and sawing schedules. Without knowing the true output at the beginning of the process, sawmill operators must produce more material to insure that

consumer demands are met. This increases waste as well as the amount of lower demand material, further lowering its price. In Maness' study, some predicted 2x4 boards were actually cut into 1x4 boards resulting in an estimated $310 loss per hour.

These issues would be difficult to resolve without a thorough mill study that tracked material flows through machine centers. Sawmill processes are complex, having both convergent and divergent flows that can loop back into other machine centers. Therefore, a mill study requires extensive manual marking to track material flow, which is time consuming and prone to error, leaving mill managers with unreliable data on which to base production decisions (Maness 1993). It also gives little indication of how machine centers interact with each other (Kline et al. 1992).

A material tracking system would allow mill managers to confirm each log's initial cutting solution from the headrig to that of the actual products produced. The machine center sawing algorithms could then be adjusted to more closely match the global optimization for the mill. According to Maness (1993), such a system should improve raw material utilization and increase a sawmill's revenue by 26 to 36 percent. It should also help match production to consumer demand, which is a key concept of consumer-driven production (Chiorescu et al. 2003; Maness 1993; Wall 1995)).

According to Maness (1993), a material tracking system could be used in conjunction with common SPC methods utilizing automatic measurements from machine centers to match the actual output to each machine center's estimates. These data could be used to adjust downstream machine center optimizers, permitting sawing schedules to better match consumers' needs, and thus, reduce waste and increase

profits. This previous research indicates that while scanning optimizers may work well individually, the lack of communication among them leads to missed opportunities to improve the entire system's efficiency (Maness, 1993; Wall, 1995).

Material tracking systems provide a better understanding of the system's operation as a whole, making decision-support systems more reliable. Currently, sawmill simulations are created using probability distributions based upon measurements taken at the machine centers, which is known as a *self-driven model* (Wiedenbeck and Kline 1994). These models tend to be costly and time-consuming By using actual data to incorporate material flow, rather than theoretical, independent distributions, a simulation model would produce more realistic results, and better analysis of the whole manufacturing system (Kline et al. 1992; Wiedenbeck and Kline 1994). However, these *trace-driven models* require a lot of material flow data and are best suited to automated material tracking systems (Wiedenbeck and Kline 1994).

2.2.2. Environmental benefit

Tracking material flow would also produce energy savings and a sawmill's carbon footprint. A one percent increase in material recovery would save US sawmills over 426.7 terajoules in annual energy usage and reduce their CO_2 Global Warming Potential increase by 9.3 teragrams, based on IPCC values (Milota et al. 2005). Combined with improved raw material utilization, this could improve the overall competitiveness of U.S. sawmills.

2.2.3. Certification benefit

Environmental certification is playing a greater role in the forest products industry as consumers demand more "green" building materials. Certification requires that materials be traced through the supply chain using a documented chain-of-custody. While the demand for certified building materials is growing, neither consumers nor producers are willing to pay the high costs associated with chain-of-custody for certification (Ozanne and Vlosky 1997; Volsky and Ozanne 1998). The software and hardware to maintain these records are costly, and for companies that wishing to process both certified and uncertified material, costs are even higher to maintain separate log inventories (Volsky and Ozanne 1998). An automated tracking system could reduce these costs, especially for companies wanting to combine log inventories.

2.3. Marking/reading methods

Logs are sometimes tracked from the forest to sawmills using radio-frequency identification (RFID) or barcode tags, but these methods have not achieved success through the sawmilling process, due largely to economic realities and the harsh operating environments of softwood sawmilling. Chiorescu et al. (2003) describes marking/reading methods, such as RFID and barcodes, as conventional tracking technologies that require the physical application of an identification tag. These methods can also be considered as deterministic identification methods, where a

predetermined identification number is attached to, or printed on, the object. We will discuss these technologies as they might be applied to softwood sawmills.

2.3.1. Radio-frequency identification

RFID systems are commonly used in supply chain management to track assets and product movements, especially in warehouses. They require RFID tags, a reader/writer device, and a computer system to store data. RFID tags are either passive or active. Passive tags receive power from the reader, and then transmit, while active tags have a battery, and continually transmit, identification information to the reader. The information, including its location, is then sent to the host computer. We will focus only on passive tag technology because it is less expensive and thus more likely to be adopted in sawmills.

Chiorescu and Grönlund (2004b) used passive RFID tags to track logs through a logyard, with the goal of comparing RFID systems to biometric identification technologies. Their study used 3409 Scots pine and Norway spruce sawlogs that were tagged on their top-ends during harvest. The identification numbers on the RFID tags were manually documented before they were scanned at the log sorting station, after which the logs were sorted and stored for three weeks. The logs were then debarked before going through the sawmill's RFID scanner. The tag readings were then checked for accuracy.

The results showed that 93% of the logs were correctly identified by the RFID system, which is not surprising because such systems are capable of reading at

distances of several feet, depending upon the environment and type of tag. RFID technology has several advantages over barcodes, such as its insensitivity to dusty conditions, and its ability to read several tags at the same time over greater distances because it does not require a direct line of sight (Chiorescu and Grönlund 2004b; Lu et al. 2006).

However, just like barcodes, RFID tracking systems are not perfect because their tags are susceptible to damage when items are moved or exposed to the elements. In the Chiorescu and Grönlund (2004b) study, over 200 RFID tags were not read or read incorrectly. According to the authors, the tags on larger diameter logs may have been too far from the RF reader. Also, RFID signals are susceptible to interference from electromagnetic noise emitted by sawmilling equipment. Finally, the moisture in the logs could have absorbed the radio signal, making it impossible to read.

While RFID tracking systems do have their advantages, many issues must be addressed before their use in sawmills becomes practical. To effectively track material flow, tags must be applied to each piece produced during log breakdown. This requires a device flexible enough to apply tags to potentially odd shaped pieces at each machine center. They also have high operating expenses as passive tags cost between 10 and 15 cents for each of the thousands of boards processed in a single shift. And, of course, tags may not survive the harsh physical handling experienced by lumber in a sawmill.

The cost to install the tag applicators, the readers, and the tags would appear to make this technology prohibitively expensive for sawmills, which leaves the logyard as perhaps the only area where RFID tags can be affordably used.

2.3.2. Barcode identification

Barcodes are commonly seen throughout many supply chains because they offer an affordable method for tracking products as a one- or two-dimensional data array read by a relatively inexpensive optical scanner. Barcodes could be applied in a sawmill either by mechanically attaching a preprinted tag, or by directly printing the code on the surface of a workpiece. Each barcode must be scanned before entering a machine center to determine a workpiece's identity and, depending on the machining process, reapplied and rescanned to maintain identification.

The greatest advantages barcodes have over RFID are their general immunity to electromagnetic noise and their lower cost tags. The obstacles for barcodes in sawmilling are the susceptibility to handling damage and the complexity of tag application, which are the same factors facing RFID systems. One additional obstacle barcodes must overcome is their susceptibility to being obscured by dust or other objects.

RFID and barcode systems have revolutionized supply chain management and tracking in many industries. However, in lumber manufacturing with its low-profit margins, these technologies may not provide the financial payback needed for viability.

2.4. Biometric identification methods

Acknowledging the weaknesses of RFID and barcode systems, researchers have begun exploring the use of biometric principles to identify individual logs and lumber. Biometric identification is defined as the recognition of individuals based on unique, measureable physiological characteristics and not on deterministic identification tags or markings (Chiorescu et al. 2003; Jain et al. 2004; Luis-Garcia et al. 2003). It can also be defined as probabilistic matching (Mansfield and Wayman 2002).

According to Jain and Pankanti (2001), biometric identification relies on two main assumptions vital for acquiring characteristics used to identify individuals. First, the relevant characteristics must remain unchanged over time and possible alteration in morphology. Second, these characteristics must be unique among different individuals. These assumptions are also known as *intraclass variation* and *interclass variation*, respectively (Jain and Pankanti 2001).

Charpentier and Choffel (2003) reviewed the basic components needed for a successful lumber tracking system using wood characteristics. Figure 3 summarizes these components in a hierarchical structure.

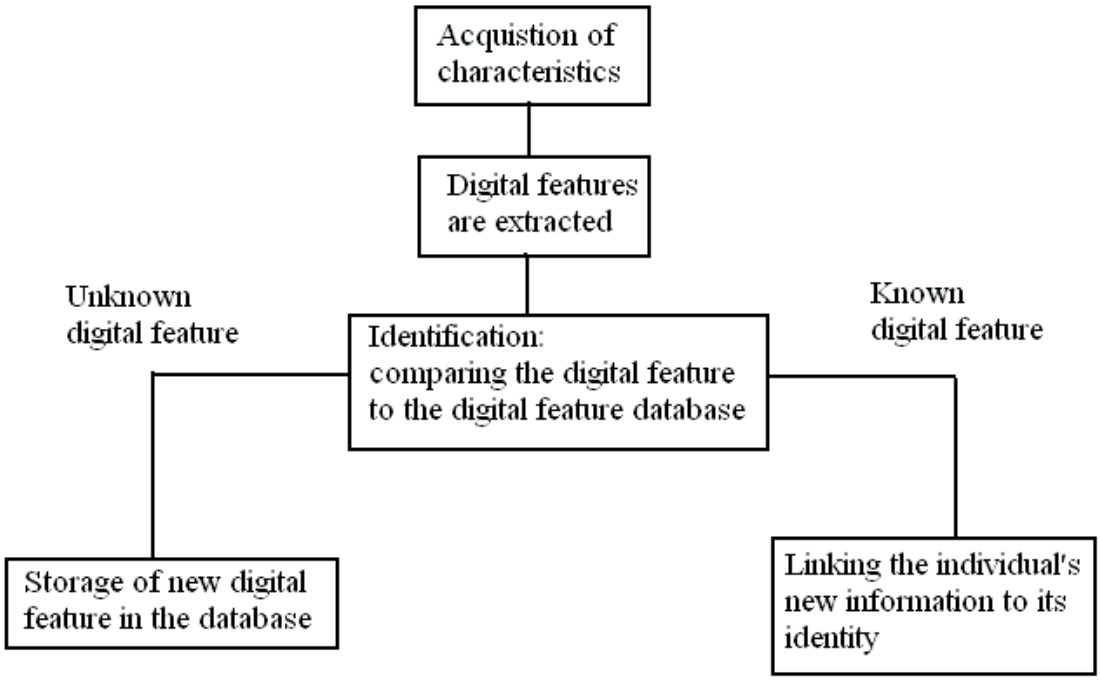

Figure 3. Four steps in tracking lumber using the inherent heterogeneity of wood. This figure after Charpentier and Choffel (2003).

Biometric methods require that wood characteristics be acquired for an individual with a technique that can convert the measurements into *digital features*, which mathematically represents the physiological characteristics.

The data can be analyzed either in its raw unaltered form or after modification by feature extraction (Jain and Pankanti 2001). Raw digital analysis can be computationally cumbersome because non-relevant data is included along with the desired digital features, and could lead to exponentially long matching times (Mansfield and Wayman 2002). It could also introduce extraneous data that obscures the relevant digital features (Jain and Pankanti 2001). Digital feature extraction reduces the data to only that needed for identification, thus reducing the ill-effects of

extraneous environmental factors that can weaken raw digital feature matching and increase matching speed (Jain and Pankanti 2001). According to Jain and Pankanti (2001), implementing an accurate digital feature extraction algorithm can be challenge.

Whether raw or extracted features are used, identification relies on acquiring one or more physiological characteristics with sufficient resolution and accuracy into a digital feature. These digital features are compared to others in a pre-existing template database using a matching algorithm, which provides a matching score that quantifies the degree of similarity between the input, or target, digital feature and the template (Mansfield and Wayman 2002). A target is thus compared to each digital feature in the database.

2.4.1. Population requirements of biometric identification systems

In a review article, Jain et al. (2004) state four criteria a characteristic must possess to achieve successful biometric identification:

- *Universality*: each individual must possess the characteristic.
- *Distinctiveness*: the characteristic is sufficiently unique to maintain identity.
- *Permanence*: the characteristic must be invariant enough to maintain identity throughout the identification process.
- *Collectability*: the characteristic must be measurable.

There are many characteristics found in wood that meet all four criteria, including knot size and location, heartwood location, annual rings, and even exterior shape. We will review previous research that uses these wood characteristics for identification.

2.4.1.1. Universality

According to Jain et al. (2004), it is important that the characteristics chosen for identification are present in each individual. In forest products, both geometric-based and pattern-based matching has been found to possess universality. Geometric-based methods rely on measuring log geometries and combining them into a unique combination of metrics used for identification. *Metrics* are scalar measurements obtained by scanners that describe the geometric shape of an individual, such as large- and small-end diameters, taper, ovality, and taper. Pattern-based matching uses a particular variability characteristic found in the individual that is not necessarily dependent upon surface geometry, such as annual ring and knot whorl patterns or location.

Pattern characteristics can be external or internal, while geometric measurements are only exterior. Geometric variability can be acquired using standard imaging equipment such as cameras. Interior variability is found within an individual using an instrument such as an x-ray scanner. Choosing a characteristic for matching can be difficult because, while exterior characteristics tend to be removed or altered at

machine centers, the measurement of interior characteristics requires expensive and complex equipment.

Chiorescu and Grönlund (2004a) used geometrics to identify debarked logs using a 3D log scanner. This scanner acquired 3D log profiles using infrared laser triangulation with scanning resolution dependent upon the feed-rate. Nine log metrics, including volume, length, area minimum diameter, middle diameter, log taper, top taper, bumpiness, relative taper, and bow, were calculated from the log scans.

After initial scanning, 773 Scots pine logs were stored in the logyard and scanned twice using the 3D scanner -- the first after two weeks and the second after two months. Each individual log's nine metrics were then matched to those in the template data, and if all the metrics fell within an arbitrary range, the log was considered a match to the one in the template. After 2 weeks of storage, the system was able to correctly match 89% of the logs, and 86% after two months.

This study demonstrates that geometric-based matching can be used for identification by employing a large number of measurement variables, or metrics. The technique was successful only because every log has a relatively distinct geometry. However, these geometric-based systems can only be used in the logyard, because the identification metrics will be altered as the logs are processed into lumber with uniform shapes and sizes (Chiorescu et al. 2003).

Pattern-based matching was explored in a study using internodal branch-whorl distances obtained from x-ray scans to identify individual boards as being from a specific Scots pine log (Flodin et al. 2008). Knot whorls are nodes of higher-density

branches characteristic in many softwood tree species, and can be considered a universal trait.

The logs were scanned at the log sorting station using an x-ray scanner and a 3D optical scanner before being processed into boards, when they were scanned again using a surface imaging system. The boards were matched, using correlation analysis, by length and internodal branch-whorl distance to the log template database. Using this method, Flodin et al. (2008) achieved a board identification rate of 95% and demonstrated that there are universal characteristics available to successfully identify log breakdown components back to their parent logs.

Both of these studies illustrate the diverse methods for identifying logs, cants, and boards using their inherent variability. Geometric-based matching, while universal and effective, cannot be applied during sawmilling because the information is removed. Pattern-based matching shows that universal characteristics can be used throughout the sawmilling process to identify individuals. In this case, the universal characteristic was internodal branch-whorl distances, which remained intact through the sawing process.

2.4.1.2. Distinctiveness

Characteristics must be sufficiently unique to distinguish an individual within a population. Chiorescu et al. (2003) investigated whether biological variation in shape could be used to identify barked logs by employing a preexisting database of 879,517 optical log profile scans acquired using laser triangulation. In their study, they

investigated which, and how many, geometric measures were needed to differentiate among individual logs. The database population consisted of 58% Scots pine and 42% Norway spruce logs scanned at several mills' the log sorting stations. The scan data included measurements of length, maximum diameter, knot placement, total taper, butt taper, bow, and ovality.

The authors developed a search algorithm (TreeSearch) to compare the scan data. They found that identification rates increased as TreeSearch included more metrics (Table 1). Different metric combinations also affected the identification rates.

Table 1. Geometric measurement variables versus the number of individuals correctly identified in both Scots pine and Norway spruce (Chiorescu et al. 2003).

Measurement parameters	Scots pine log identification rate (n = 510,120)	Norway spruce logs identification rate (n = 369,397)
Diameter + length	3%	3.90%
Diameter + length + butt taper	64%	68%
Diameter + length + butt taper + bumpiness	98%	99%

These results demonstrate that distinctiveness is important in biometric identification. There must be sufficient variability in the characteristic to determine the identity of individuals, which can be a challenge, especially when simplifying measurements into several scalar metrics. In this case, the identification results increased significantly when butt taper and bumpiness data were added to the metric combinations.

This demonstrates that some characteristics provide more useful information than others and that choosing which characteristics to use is critical when developing an identification system. For instance, including ovality did not improve identification rates. On the other hand, the study also shows that no single characteristic provides enough information for error-free identification.

The usefulness of including more variables is also demonstrated in the Flodin et al. (2008) x-ray identification study that found significant improvements in identification using a log length filter to reduce the number of potential template matches, which improved the probability of obtaining a true match (Jain et al. 2004). The study also confirms the benefit of using multiple characteristics to identify parent/child relations discussed by Luis-Garcia et al. (2003) and Jain et al. (2004).

Chiorescu et al. (2003) also used the filter concept by creating three log diameter classes from 3000 semi-randomly selected log scans (1000 in each class) and used their TreeSearch algorithm to match individuals within each diameter class using the diameter, length and butt taper metrics. The results are shown in Table 2.

Table 2. Using three geometric measurement variables, the number of individuals identified increased with increasing diameter class (Chiorescu et al. 2003).

	Diameter + length + butt taper	
Diameter class	Scots pine log identification rate (n = 1500)	Norway spruce log identification rate (n = 1500)
Small diameter (160 to 190 mm)	76%	86%
Medium diameter (230 to 260 mm)	90%	92%
Large diameter (300 to 330 mm)	99%	99%

By separating the individuals into three diameter classes, identification rates were significantly improved. The probability of having indistinguishable, or twin logs decreased as the log population decreased, which improved results and shows that population size is important in biometric identification because, as the test population increases, the probability of having "twin" samples increases (Chiorescu et al. 2003; Jain et al. 2004).

Chiorescu et al. (2003) also identified several weaknesses in the distinctiveness requirement when using log scans for identification. Large logs with bark have greater geometric variability and are therefore more likely to provide correct matches. Additionally, debarking logs changes the geometric measurements, violating the permanence requirement (Jain et al. 2004), which makes matches between the two types of scans less likely. Another drawback to implementing this tracking scheme in Pacific Northwest mills is the necessity of installing another log scanner at the log-yard receiving station.

Additionally, distinctiveness can vary among species. In this case, Scots pine and Norway spruce logs differed slightly when matched with the same metrics. This is largely due to the genetic differences between the two species as Norway spruce tends to have more butt taper and a rougher bark surface than Scots pine (Chiorescu et al. 2003), and emphasizes that care must be taken when selecting the characteristics to use for a given species. Variability characteristics should not be generalized to other species; a given species must be extensively studied to get the best identification results.

2.4.1.3. Permanence

Permanence, or the ability of a characteristic to retain its distinctiveness over time, is vital to any identification system's success. The issue with wood characteristics in a sawmilling environment is twofold. As logs are processed into boards, characteristics are removed at each machine center; thus, morphology changes must be accounted for when choosing a variability characteristic. Also, because wood is a hygroscopic material, characteristics will change as moisture content changes (e.g. shrinking and swelling).

Chiorescu and Grönlund (2004b) addressed the issue of morphological change by matching individuals' barked log scans to their debarked scans. They scanned logs with their bark at the log sorting station using a 3D log scanner to calculate length, volume, top volume, minimum diameter, middle diameter, maximum diameter, diagonal diameter, bow, mean taper, butt taper, bow position, top ovality, top ovality

angle, and middle ovality angle. The logs were then debarked after 3 weeks of storage, and scanned again. To match the barked log scans to the debarked log scans, a "bark reduction" algorithm was used that inferred the log's debarked metrics using the barked logs' initial scanning data. These inferred metrics were used as the matching templates to compare to the actual debarked log scans.

The results showed that, even with the bark reduction algorithm, only 57% of the logs were correctly identified, which demonstrates that permanence is vital to successful biometric identification. Even after addressing the removal of bark using their bark reduction algorithm, the results failed to compare favorably with previous studies. While bark provides a unique surface for identification, it is not a permanent characteristic in a sawmill and usable information is reduced as it is removed (Chiorescu and Grundberg 2001).

Similarly, when comparing the Chiorescu et al. (2003) identification results on barked log scans to the Chiorescu and Grönlund debarked log study (2004a), the debarked log identification results are better in the small and medium diameter classes and worse in the large diameter class (Table 3). This is likely due to the higher degree of variability found in larger logs (Chiorescu et al. 2003). In the Chiorescu and Grönlund study (2004a), debarked logs were scanned at the log sorting station and sawmill infeed, and even without bark's added variability, a large proportion of logs were correctly identified. However, a problem arises when scans of barked log taken at the sawmill's log sorting station must be matched to scans of the debarked log taken at the sawmill's infeed.

Table 3. Comparing identification results from barked logs to debarked logs (Chiorescu et al. 2003; Chiorescu and Grönlund 2004a).

Diameter class	Barked Scots pine log identification rate	Debarked Scots pine log identification rate
Small diameter (160 to 190 mm)	76%	81%
Medium diameter (230 to 260 mm)	90%	92%
Large diameter (300 to 330 mm)	99%	93%

Flodin et al. (2008), who used x-ray scans to match boards to their parent logs, also showed that dynamic changes in individual logs can be addressed during processing by considering the change in board length after log processing. As logs are processed into boards, internal stresses can be released, resulting in board lengthening, which confounds a "parent" log to "child" board length comparison. Flodin et al. (2008) found that board lengths increased an average of 1.2 cm with a standard deviation of 1.6 cm; to account for this change, they applied a correction factor to their matching algorithm. This resulted in a 95% identification rate.

A study by Charpentier and Choffel (2003) also addressed the issue of permanence when acquiring microwave characteristics of wood. Their objective was to determine if microwave scans of board surfaces contain enough variability to identify individual boards using a pattern-based matching method.

Microwave sensors were used to measure wood dielectric properties, which vary mainly with moisture content, density, and slope of grain. These characteristics could be used to match a sample in a database of digital features, assuming that

moisture content differences were minimized. Charpentier and Choffel's (2003) goals were to determine whether there were detectable differences among four individuals, and if the measurements were repeatable for a single individual. The third goal was to determine the effect of crosscutting and planing on the microwave measurements.

They used Maritime pine samples (2000 x 120 x 27 mm) chosen to maximize physical differences, mainly knot placement and slope of grain. Samples were equilibrated to 14% moisture content to reduce the effect of moisture content during scanning. Boards were scanned along their length at the centerline with readings made every 7 mm. The digital features were compared using correlation analysis with the authors arbitrarily choosing correlations above 0.90 as constituting a correct match.

Charpentier and Choffel's (2003) found the scanning measurements to be highly repeatable with correlations ranging from 0.98 to 0.99 over four scans of the same board. This indicates that the characteristics were consistent over a short period of time, although the exact times between scans were not given. The results indicate that the permanence requirement was met for biometric identification under ideal conditions.

Charpentier and Choffel (2003) also experimented with microwave measurements as boards were cut shorter. They found that correlations decreased from 1.00 when only 200 mm was removed to 0.93 when 800 mm was removed. These high correlations indicated that the longitudinal characteristics were very stable along a board's length, and according to the author's correlation cutoff, would be

considered correct matches. These results seem reasonable because the boards did not change in thickness, only length.

During planing, the digital feature correlations decreased from 0.99 when the boards were 25 mm thick (unplaned) to -0.07 when they were planed to a thickness of 10 mm. The planing was confined to only the side that was measured originally, which showed that matching becomes more difficult with increasing morphological changes. According to the Charpentier and Choffel's (2003), this was most likely due to a changing slope of grain, but it could also result from angled or partial knots as well as moisture content differences.

The Charpentier and Choffel's (2003) study demonstrated that variability along the grain has the potential for biometric identification and that wood meets the biometric requirements presented by Jain et al. (2004) and Luis-Garcia et al. (2003) under controlled laboratory conditions. However, it also showed that identification becomes difficult with the significant morphological changes that occur when boards are planed by only a few millimeters. This would become an issue when tracking logs or cants because microwave sensors cannot scan the interior of larger pieces and surface readings will change significantly as material is removed. Also, the variability of moisture content within and among sawlogs must be addressed because high moisture content could mask characteristics for during acquisition (Charpentier and Choffel 2003). However, the technique appears to be useful for identifying pieces close to their final dimensions and moisture content.

2.4.1.4. Collectability

As the above research has demonstrated, there are many external and internal variability characteristics found in wood that could be used for identification of individuals; but to do so, they must be measured with sufficient resolution and accuracy. For example, the study by Chiorescu et al. (2003) showed that log identification rates increased when higher-accuracy and higher-resolution log scanners were used. While scanning systems might be capable of tracking wood material in some cases, they may not have the required accuracy or resolution to allow for consistent identification of individual pieces through the whole breakdown process (Chiorescu et al. 2003, Maness 1993).

Another example is the Charpentier and Choffel (2003) study, which demonstrated that accuracy and resolution are important to microwave measurements. They provided evidence that their microwave system was accurate, but found little additional information obtained with resolutions greater than 5 mm. They used a scanning resolution of 7 mm to compromise between resolution and data overload.

The sawmilling process itself could complicate acquiring accurate measurements. Depending on the acquisition method, sawdust can distort or mask measurements. Physical damage caused by pieces hitting each other or other objects could also produce changes as well. One must decide how sensitive, or how much resolution is needed to obtain useful information. Too much detail could decrease recognition rates as the system might detect dust and physical damage instead of actual characteristics, while reducing the level of detail could alleviate the effects of

some environmental factors, it might also adversely affect high identification rates. This, however, would depend on the sawmill and how it processes material.

2.4.2. Biometric identification using end-grain

We have discussed a number of studies that explore biometric identification of logs and boards. Their findings indicate that wood possesses sufficient variability for biometric identification; however, an effective system depends largely on using characteristics that change very little during processing. Such a system could use the proposed techniques of Chiorescu et al. (2003; Chiorescu and Grönlund 2004a, 2004b) for tracking logs to the sawmill infeed, and those from Charpentier and Choffel (2003) for tracking boards; but neither system can identify individual pieces as they are processed from the headrig to the trimmer, where boards are cut to their final length. This implies that a successful tracking material will require the measurement of several biometric digital features to maximize variability while using characteristics that change very little.

Probably the most suitable surface for identification would be the cross-section, or end-grain because it is not purposely altered until the board is trimmed. However, there is currently no research on end-grain characteristics for biometric identification. A major economic advantage to using end-grain for log and board identification is that camera systems, which are a practical and affordable alternative to x-ray and microwave scanners, can be placed at each machine center. These camera systems could image the end-grain of logs before and after they are sawn by

the headrig, after they are sawn by the gangsaw, before and after they are processed by the edger, and before being cut at the trimmer. As a computer identifies each piece by matching its end-grain pattern, a history of each piece's flow through the sawmill could be built.

There are several end-grain characteristics, affected by both genetic and environmental factors that could contribute to the identification of individual pieces. As with all temperate zone softwoods, annual-growth rings are universal in Douglas-fir and vary by the proportion of earlywood to latewood, the number of rings per inch, and eccentricity. These factors will vary due to a tree's growing region, local weather patterns, fertilizations, and local genetic characteristics. Also, the amount of heartwood, the non-living inner core of the tree, is variable and can help distinguish individuals when its color is distinguishable, as it is in Douglas-fir. The overall surface texture of end-grain is another universal characteristic that may contribute to identification. Finally, the presence of knots on the surface can also aid in identification because, while they will not be present on every end-grain surface, when present, they produce a distinct pattern.

There are, however, some wood properties that can affect characteristic permanence. Changing moisture content is known to affect the dimensionality of wood (Panshin et al. 1969). As moisture content in wood decreases, the volume decreases causing annual rings to constrict. At some point, the internal stresses will cause cracking. It is also known that decreasing moisture content will reduce the

contrast in wood. Annual rings and heartwood become less visible, making these characteristics more difficult to detect.

3. MATERIALS AND METHODS

This section describes the logs used for this study, and the steps in capturing their end-grain images. We will then describe the methods used to analyze end-grain image suitability for biometric identification.

3.1. Material description

Log cross-sections were taken from untreated 20-foot Douglas-fir (*Pseudotsuga menziesii*) utility pole sections. The poles were shaved at McFarland Cascade Pole & Lumber Company, which involves removing all bark and protrusions, such as branches stubs, from the logs, while limiting wood fiber loss. These utility poles were used because of their availability from an unrelated study. The samples measured between 8.13 and 10.93 inch-diameters on the small-end and between 9.29 and 12.43 inch-diameters on the large-end (Table 4). For the other study, they were stored outside for 4 to 8 weeks during the summer of 2009, and watered constantly using a sprinkler system to prevent dimensional change and splitting.

Table 4. Maximum, minimum, and average diameter values for the 60 Douglas-fir utility poles.

Statistical Measure	Small-end diameter (inches)	Large-end diameter (inches)
Minimum	8.13	9.29
Maximum	10.93	12.43
Average	9.44	11.14

Cross-sections three-inches in length were cut from the top and bottom of each pole. The sections were labeled with log identification numbers that also indicated if they were taken from a pole's top or bottom. The 120 sections were sealed in plastic bags along with added water, and placed in a freezer to prevent checking and cracking for the two weeks of sample collection.

3.2. Imaging the samples

The samples were imaged using a Nikon D90 camera with a Nikon 50 mm f/1.8 lens attached to an aluminum-framed camera fixture, set at a height of 52 inches (Figures 4a and 4b). Two 50-watt, 120-volt halogen floodlights were used to provide consistent lighting. The camera was controlled by computer using Nikon Control Pro 2 imaging software. For all images, the camera was set to manual mode, using a 1/100-second exposure and f/3.2 aperture, taking 12-bit per channel color images. We used 12-bit images to minimize in-camera data compression effects. The ISO exposure was set to 200, and the camera's autofocus was used to ensure consistent image sharpness. The focal length, or distance from the lens to the sample, was 49 inches.

(4a) (4b)

Figure 4. The experimental setup for image capture (Sample cross-sections were imaged before they could develop splits).

The camera provided a live video feed of the image area to the computer, which was used to align, or register, each sample in the image area using cross hairs superimposed onto the video feed. The pith of each sample was placed at the center of the cross hairs, and the samples were marked with four reference marks on the outer circumference, corresponding to the crosshairs as shown in Figure 5.

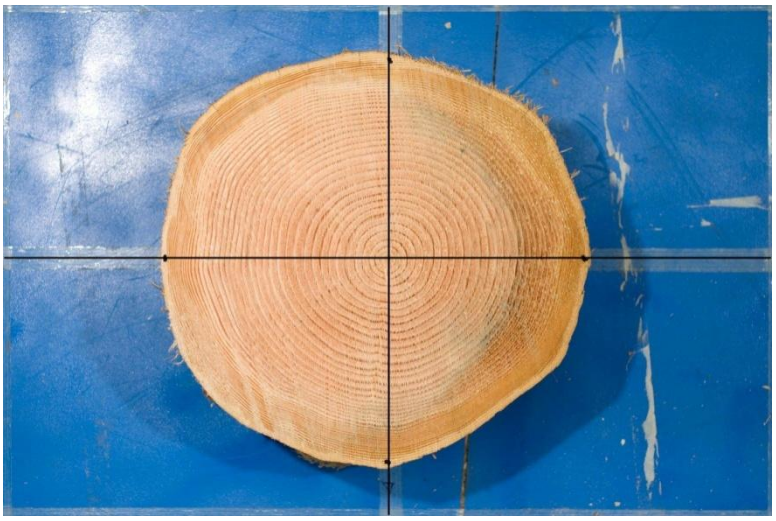

Figure 5. An example of the image overlay allowing for consecutive image registration.

The samples were randomly imaged three times over a span of three days, acquiring the 120 registered cross-section images each day. The reference points were used to align the samples during the second and third repetitions. This registration technique was used to insure all images had the same center point and a similar orientation. The samples were stored in the lab during this period. Care was taken to insure consistent orientation of the samples during imaging. Reference images were also taken of each cross-section with a ruler to measure the pixel resolution of the images, which were 200 pixels per inch (ppi).

3.3. Preparing the images

To provide compatibility with the image matching algorithm, the blue background was replaced with a consistent 50% grey using Adobe Photoshop. The

images were then converted to 8-bit grey-scale by averaging the color channels, after which they were cropped around the end-grain to minimize the background. An example image is shown in Figure 6.

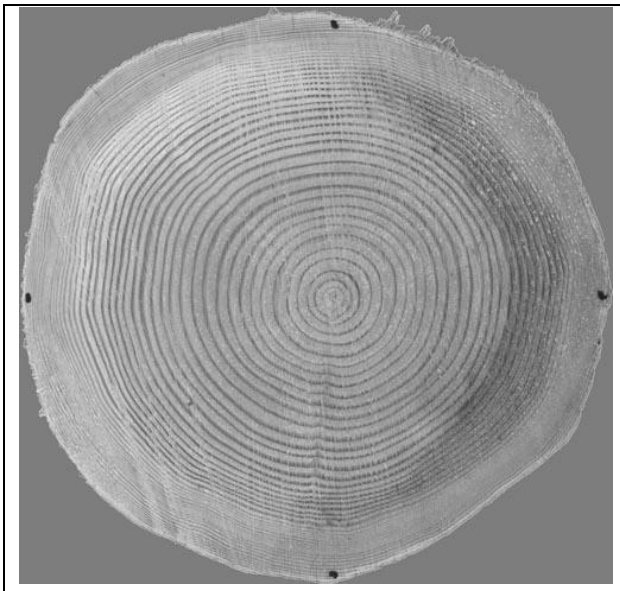

Round image 103B from day 1

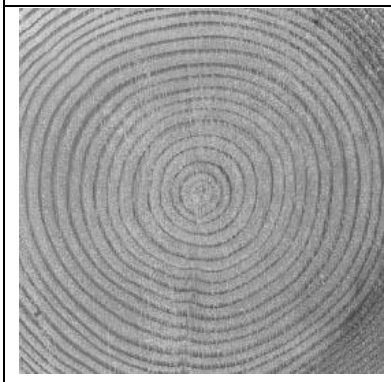

Cant image cropped from round image above

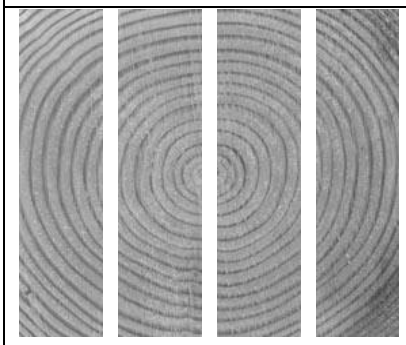

Board images cropped from cant image above

Figure 6. Image sequence developed from the original cross-section image for each image set. The same procedure was used to develop the second and third day images.

The images were placed into three groups with each group representing the images taken on a particular day, so that each set had one image of each cross-section and were labeled in relation to the day they were imaged. The center of each image was recorded on a computer using two straight lines placed on the four points marked on the samples during imaging (Figure 5). This insured that the images from each three imaging sessions were registered to the corresponding image in the other groups.

The images simulated the three stages of log breakdown: rounds (unsawn logs), cants, and boards. The round images simulated the imaging of the log end-grain in the logyard. Copies of the round images were cropped into 6.5-inch by 6.5-inch 4-sided cants, which simulate headrig processing. The images were cropped using the center of each image as the reference point. Finally, cropping four 5.5-inch by 1.5-inch images from copies of each cant image created the board images, simulating the gangsaw processing. This resulted in three image sets, each with three subsets of images consisting of 120 rounds, 120 cants, and 480 boards for each day (Table 5).

Table 5. Image crops organized into their respective image days.

Image Day 1 (N = 120)	Image Day 2 (N = 120)	Image Day 3 (N = 120)
Day 1 Rounds (n = 120)	Day 2 Round (n = 120)	Day 3 Round (n = 120)
Day 1 Cants (n = 120)	Day 2 Cant (n = 120)	Day 3 Cant (n = 120)
Day 1 Boards (n = 480)	Day 2 Boards (n = 480)	Day 3 Boards (n = 480)

3.4. Analysis of biometric identification performance

The biometric identification method of analysis presented by Jain et al. (2004) and Luis-Garcia et al. (2003) relies on signal detection theory; in which an individual is, or is not, matched to a given digital feature template. This results in a binary decision space. Through the use of a matching algorithm, the degree of similarity between the individuals being matched (called targets), and templates can be quantified. This measure is known as a matching score, which, in our case, is an image correlation between the pixel values contained in the target to the template pixel values. Because identification systems iteratively match every target to every template, many thousands of matching score observations can occur during a single matching run. Every target being matched will return a genuine matching score if the target's template is in the database, or an impostor matching score if the target's template is not in the database. This results in two independent, continuous, matching score distributions.

3.4.1. Signal detection theory

A genuine match is defined as an individual that is matched to its correct identity, or template; called a *true positive* (TP). An impostor match is an individual that is not matched to another, different identity, or template; called a *true negative* (TN). In an identification system, a match is attempted for every individual for every template in the database. Ideally, the matching scores from the genuine and impostor distributions do not overlap, thus precluding mistaken identifications (Figure 7).

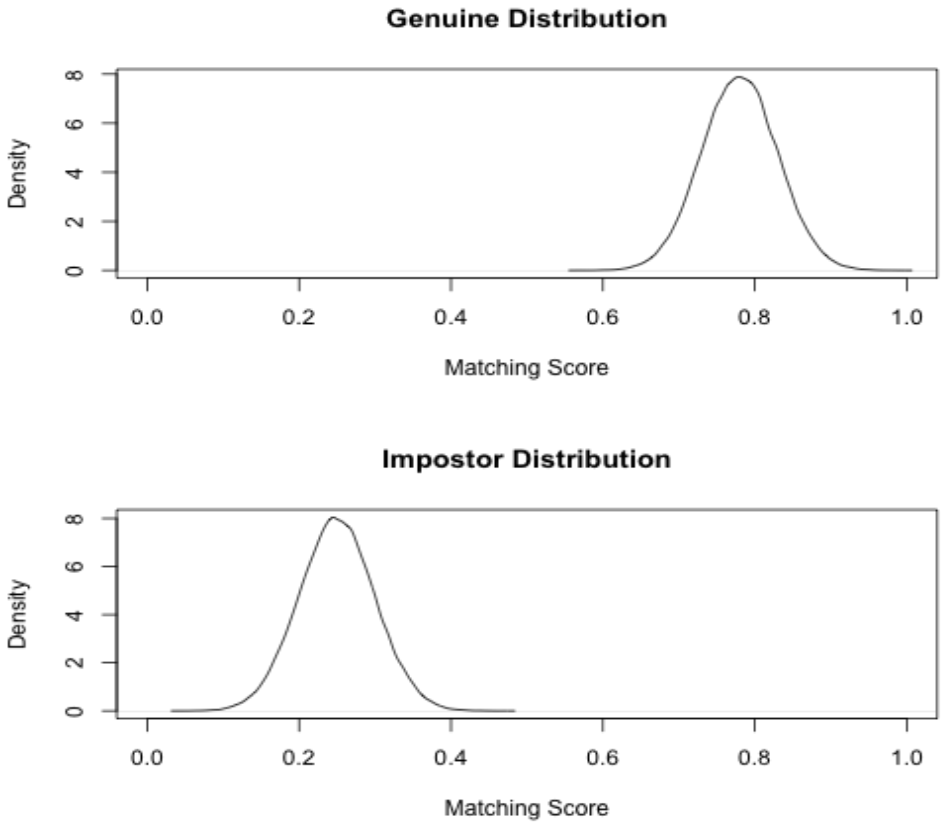

Figure 7. The genuine and impostor distributions showing distinct differences between digital feature matching scores.

However, in the event that the genuine and impostor distributions overlap, there are two additional possibilities: *false positive* (FP) and *false negative* (FN). A false positive is an individual who is mistakenly matched as another individual, while a false negative is an individual who is mistakenly not matched to its template. These are commonly known as Type I and II errors, respectively.

A system that uses matching scores to determine a match must define an arbitrary decision threshold that defines the level of misidentification risk. Scores

higher than the threshold are considered positive matches, while lower scores are considered negative matches.

Table 6 shows a contingency table of the four possible identification classifications for a given threshold value. The columns contain the genuine and impostor distributions and the rows contain the success and failure rates for each distribution. The results are fractional (TPF + FNF = 1, and FPF + TNF = 1). These proportions change as the threshold value increases or decreases. The graphical representation of these possibilities is shown in Figure 8. The threshold value set at 0.5 shows that, while the majority of true positive matches occur, there are some false positive matches.

Table 6. Contingency table showing the possible identification results for a group of individuals, given a threshold value which defines a "high" and "low" score.

	Genuine identity	Impostor identity
High matching score	**True positive fraction** (TPF) $= \frac{True\ positives}{Total\ positives}$	**False positive fraction** (FPF) $= \frac{False\ positives}{Total\ negatives}$
Low matching score	**False negative fraction** (FNF) $= \frac{False\ negatives}{Totals\ positives}$	**True negative fraction** (TNF) $= \frac{True\ negatives}{Total\ negatives}$

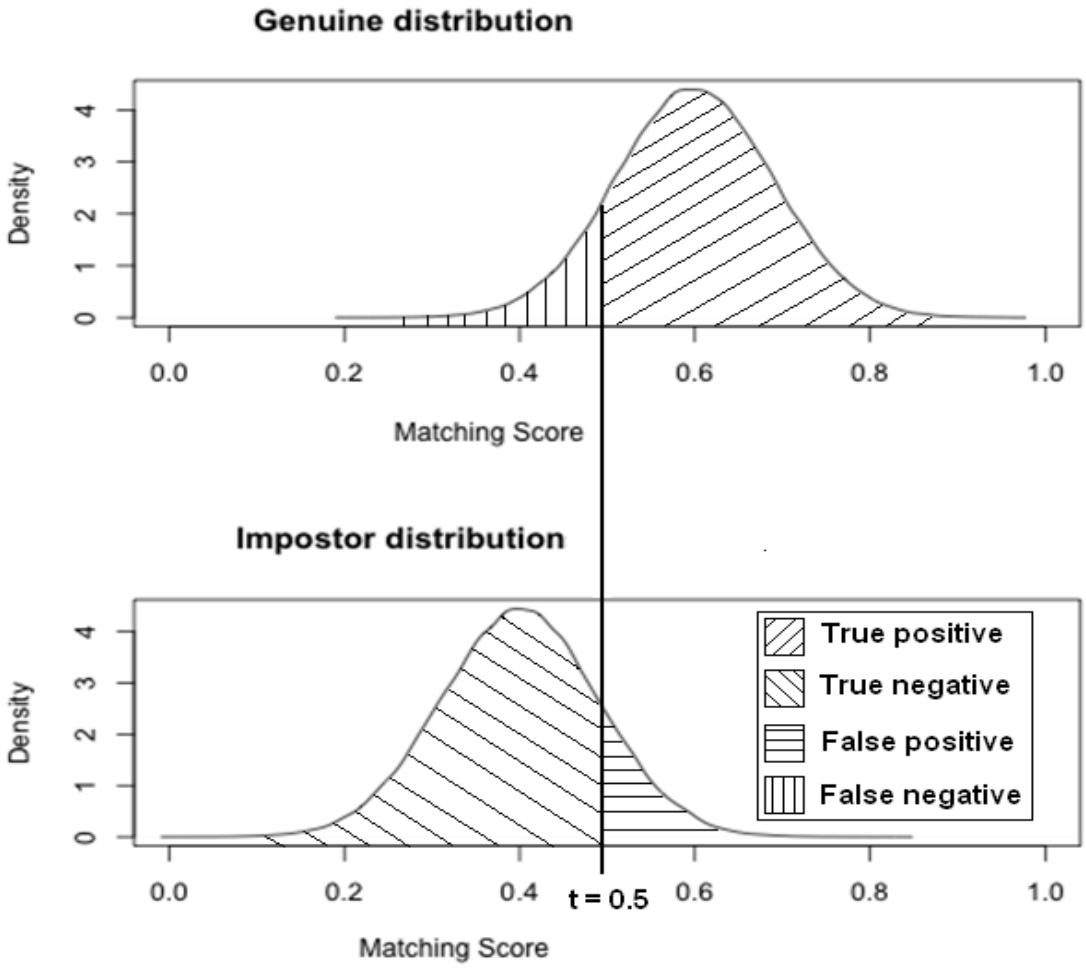

Figure 8. With a threshold value set at 0.5, 75% of the true positive matches are made, but there are 25% false positive matches.

From these contingency tables, another important value can be calculated; the accuracy of the system at a given threshold level. Accuracy is defined as the number of true positives plus the number of true negatives over the total number of positive and negatives. The equation is shown in (1).

$$Accuracy = \frac{True\ positives + True\ negatives}{Total\ positives + Total\ negatives} \qquad (1)$$

The generic model for a biometric identification system is shown in (2) (Jain et. al 2004; Luis-Garcia et al. 2003). Given a digital feature, known as a target, X_Q, the system determines the identity of an individual, I_k, where k Є {1, 2,…, N}. The target is input into the matching algorithm, S, and is matched to each digital feature in the database, known as templates, $S(X_Q, X_{Ik})$. This function returns a matching score that measures the degree of similarity between the input digital feature and each template digital feature. There are two possibilities for each comparison between the input digital feature and the digital feature database:

$$X_Q \in \begin{cases} I_k, & if\ max_k\{S(X_Q, X_{Ik})\} \geq t, k = 1,2,\dots,N \\ I_{N+1}, & otherwise \end{cases} \quad (2)$$

X_{Ik} is the digital feature template of the individual, I_k, in the database, $S(X_Q, X_{Ik})$. The variable, t, is the threshold value that indicates which matching score must be met to be considered a positive match. If multiple matching scores are above the threshold value, then the highest value is used.

3.4.2. ROC Analysis

To fully analyze the binary decision space, the resulting true positive fraction and false positive fractions are obtained by varying the threshold value between 0 and 1. The TPF and FPF are then calculated at each threshold value, and plotted against each other. These plots are known as a *receiver operating characteristic*, or ROC, curve.

The ROC curve is a useful method for visualizing classifier performance as it displays both the costs and benefits of a threshold function. An ROC curve plots the results of a contingency table without being sensitive to differences in the classifier populations, which makes them useful in biometric identification studies with differences of up to 6 orders of magnitudes in population size (Fawcett 2006; Jain et al. 2004).

ROC curves rank the matching scores from lowest to highest, and calculate the proportion of true positive values relative to the proportion of false positive values determined by a threshold value. This can be accomplished with either calibrated probability matching scores or uncalibrated relative matching scores (Fawcett 2006). With ROC methods, matching algorithms using raw, uncalibrated, matching scores can be analyzed, so long as the scores indicate a reliable degree of similarity between the target and the template. However, because the scores are relative to the algorithm, the results cannot be compared to other studies using a different matching algorithm (Fawcett 2006). Any measured metric, such as accuracy, will indicate performance relative to the analyzed matching algorithm, not a true probability that can be extrapolated to other studies (Fawcett 2006).

The diagonal line in the ROC space (Figure 10) represents completely overlapping distributions, where no distinction between genuine and impostor populations is possible. Thus, any curve found above this diagonal indicates the algorithm is able to differentiate members of the two populations to some extent. The further up and to the left the ROC curve, the more successful the algorithm is at

identifying individuals. In fact, the point on a curve that is furthest up and to the left is the threshold level that provides the highest accuracy of the system.

An important characteristic associated with the ROC curve is the Area Under the Curve (AUC), which is calculated as the proportional area under the ROC curve and, therefore, ranges between 0 and 1.0. The AUC gives a single value that indicates the expected performance of the system and measures the probability that a randomly chosen genuine individual will have a higher matching score than a randomly chosen impostor individual, which is equivalent to the Wilcoxon test of ranks (Fawcett 2006). An ROC curve following the diagonal line will have an AUC of 0.5, while the ROC curve in Figure 10 has an AUC of 1.0.

In an ideal binary decision space, where the genuine and impostor distributions do not overlap (Figure 9), an ROC curve will be two perpendicular lines (Figure 10). The ROC curve has four decision thresholds for reference. When the threshold is at 0, the TPR is 1, while the FPR is 0. Following the threshold levels along the ROC curve shows a decrease in the FPR, while the TPR remains constant. As the threshold increases beyond the impostor distribution ($t = 0.5$), the FPR decreases to 0. At this point the accuracy of the system is at its highest level of 100%. However, as the threshold increases into the genuine distribution, the TPR decreases to 0, and the accuracy returns to 0. The figure indicates no risk at any threshold level for an error to occur; the AUC is 1.0.

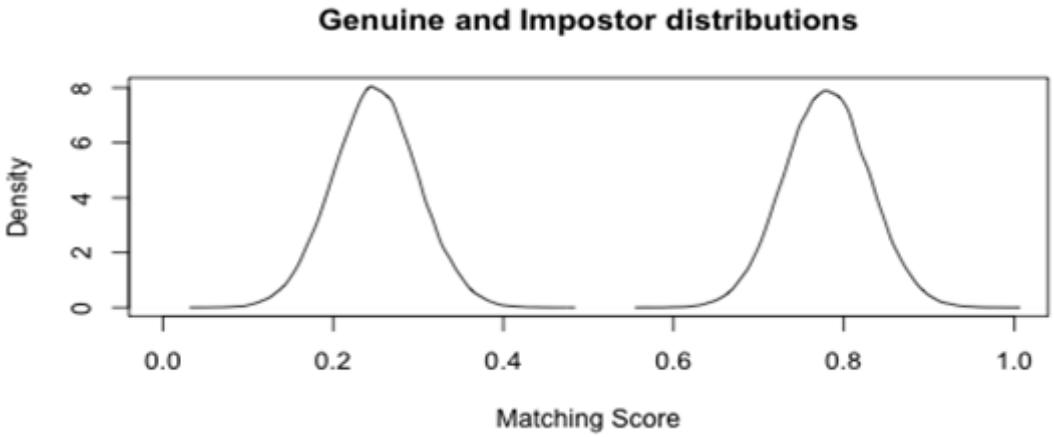

Figure 9. Completely separated genuine and impostor distributions indicating that the digital features between individuals are significantly unique.

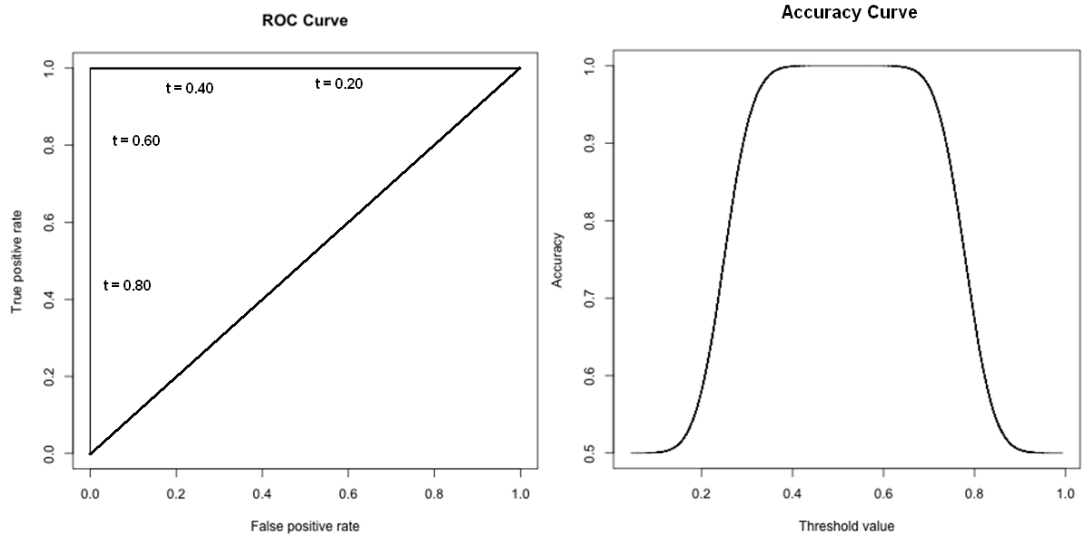

Figure 10. The ROC and accuracy curves of non-overlapping distributions. The ROC curve indicates a "perfect" classification performance. The accuracy curve shows that the highest performing threshold lies between 0.45 and 0.55, with an accuracy of 1.0.

As the distributions overlap, the matching algorithm is less able to distinguish between the genuine and impostor distributions, such as those shown in Figure 11.

The resulting ROC curve is shown in Figure 12, with its associated accuracy curve. Note that the ROC curve is flatter than the previous ROC curve indicating a poorer performing system. If the threshold value is very high, 0.8 for example, there would be almost no false positives, but at the cost of identifying fewer true positives. Similarly, a low threshold value would produce more true positives, but at the cost of more false positives. The point at which this system performs best is at the threshold value of 0.55

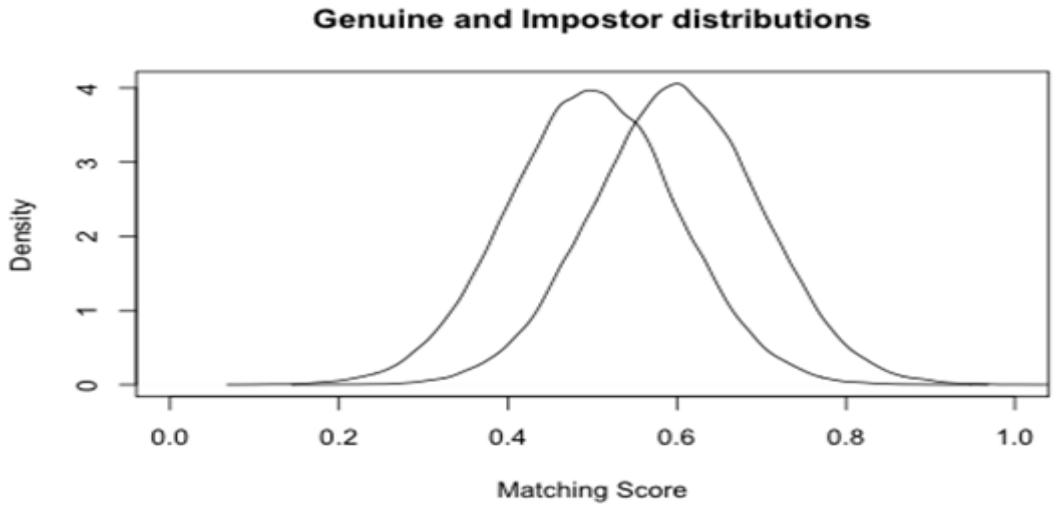

Figure 11. Overlapping genuine and impostor distributions indicated digital features that are difficult to distinguish.

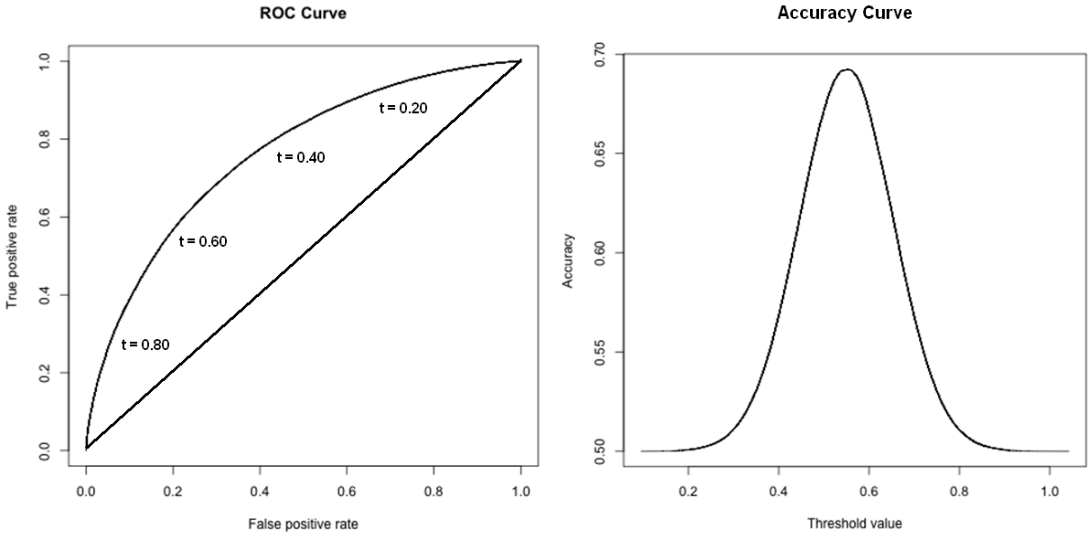

Figure 12. The ROC and accuracy curves of overlapping distributions. The ROC curve shows the cost of applying a given threshold value. The accuracy curve shows that the highest performing threshold is at t = 0.55, with an accuracy of 0.69.

The charts and statistics were created using R, an open-source language and environment for statistical computing (Version 2.10.1). The ROC curves were created using the R software package ROCR (Version 1.0-4).

3.5. Matching the images

The proprietary image matching algorithm used to match end-grain images was developed by Adin Berberovic and uses image correlation on raw images, i.e. no digital feature extraction. The algorithm iteratively compared a target's grey-scale pixel intensity values to those of each image template in the database, and returned a matching score for each comparison. A matching score is the ratio of correlated intensity values between the target and template image.

Table 7. The board-to-cant and cant-to-round matching combinations used to match end-grain images.

Run	Target images	Matching templates
Matching Scenario 1	Day 2 boards	Day 1 cants
Matching Scenario 2	Day 3 boards	Day 2 cants
Matching Scenario 3	Day 2 cants	Day 1 rounds
Matching Scenario 4	Day 3 cants	Day 2 rounds

We matched four combinations of the three image sets to create the scenarios shown in Table 7. This allowed us to determine how permanent these characteristics were with time and changing ambient conditions that affect moisture content by comparing images taken between days 1 and 2 and days 2 and 3. End-grain images taken on the same day were not matched because they would be identical. The matching algorithm would consume weeks of computer time for each scenario at the original 200 ppi, so the pixel resolution for the board-to-cant matching images was reduced to 100 ppi and the cant-to-round matching images were reduced to 50 ppi to reduce computer times to reasonable levels.

To maintain independence between the genuine and impostor distributions, it is standard practice to remove a subset of individuals from the database, but still included them in the search as targets (Mansfield and Wayman 2002). For the board-to-cant matching scenarios, 400 of the 480 board images in the target population came from the 100 cant images in the template population for Matching Scenarios 1 and 2. The remaining 80 board images came from 20 cant images randomly chosen to be the impostor population; thus, 480 boards were matched to 100 cants in the template

database. This design produced 400 genuine matching scores and 8000 impostor matching scores for each scenario.

For the cant-to-round matching scenarios, 120 cants were matched to 100 rounds in the template database. Of the 120 cants, 100 were genuine samples whose images were included in the template database and 20 were impostors because their images were not included in the template database, which resulted in 100 genuine and 2000 impostor matching scores for each matching scenario.

4. RESULTS

In this section, the results for the board-to-cant and cant-to-round matching scenarios are summarized.

4.1. Board-to-cant matching results

The results for Matching Scenario 1 (Day 2 boards to Day 1 cants) are summarized in Table 8. The genuine and impostor matching scores were statistically different from each other (Welch two sample t-test p-value < 0.0001). Matching Scenario 2 (Day 3 boards to Day 2 cants) results are also summarized in Table 8. The genuine and impostor populations were also statistically different from each other (Welch two sample t-test p-value < 0.0001).

The scores varied between the matching scenarios, with a mean difference of 0.0431 for the genuine matching scores and 0.0174 for the impostor matching scores. This decrease was statistically significant (Welch two sample t-test p-value < 0.0001). The variance of the population increased significantly between the two matching scenarios, from 0.01045 to 0.01846 for the genuine matching scores (Fisher's f-test p-value < 0.0001) and 0.00424 to 0.00564 for the impostor matching scores (Fisher's f-test p-value < 0.0001).

Table 8. Statistics describing the genuine and impostor matching scores for each board-to-cant matching scenario.

	Matching Scenario 1		Matching Scenario 2	
Distribution	Genuine n = 400	Impostor n = 8000	Genuine n = 400	Impostor n = 8000
Mean	0.7556	0.2419	0.7125	0.2245
Median	0.7718	0.2439	0.7371	0.2293
Variance	0.01045	0.00424	0.01864	0.00564
Range	[0.4414, 0.9391]	[0.0519, 0.5620]	[0.2689, 0.9355]	[0.0535, 0.5721]

Figure 13 displays the histograms of the genuine matching scores for each board-to-cant matching scenario. Both show a negative skew. Matching Scenario 2 shows more negative skew than Matching Scenario 1. Figure 14 shows the histograms of the impostor matching scores for each matching scenario, showing positive skew. Figure 15 shows the normal QQ plot for the genuine distributions. Deviations in normality can be seen at the upper end of the plots for both genuine distributions, but both were reported as normal. Figure 16 displays the normal QQ plot for the impostor distributions. Deviations in normality are also seen at both ends of these plots, but both were reported as normal.

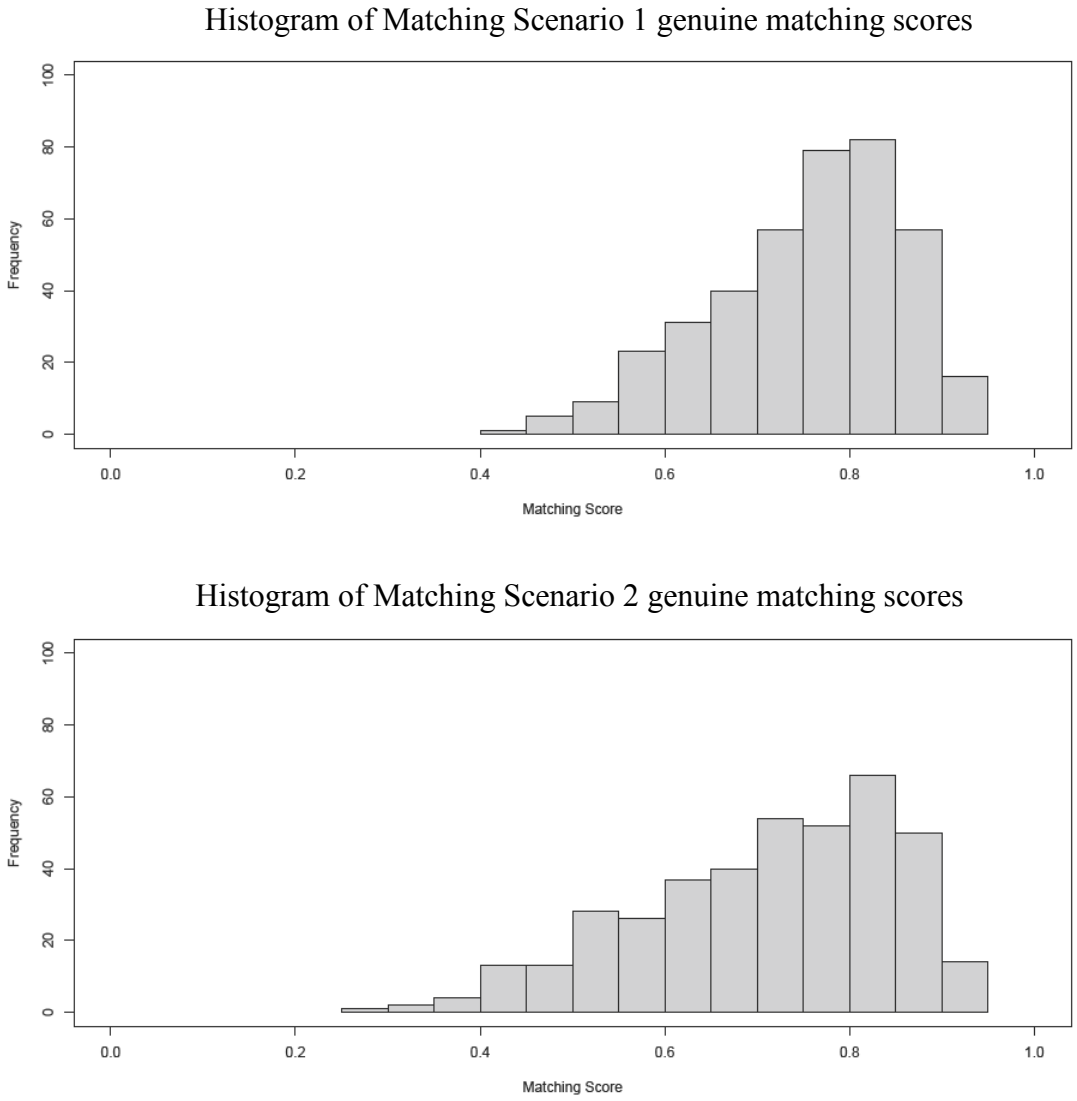

Figure 13. Histogram of the genuine matching scores for both board-to-cant matching scenarios, each showing negative skew (n = 400).

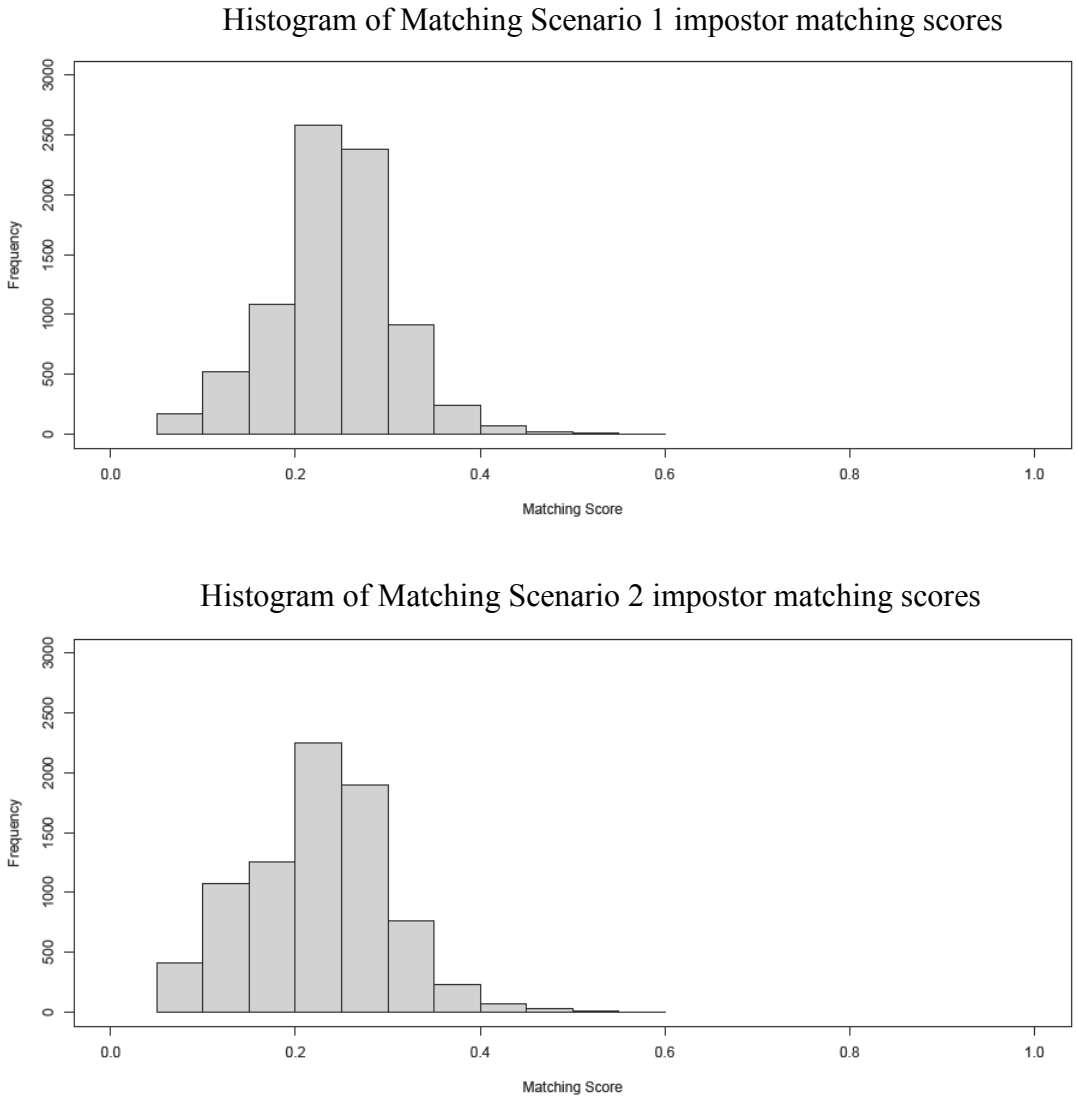

Figure 14. Histogram of the impostor matching scores for both board-to-cant matching scenarios, each showing positive skew.

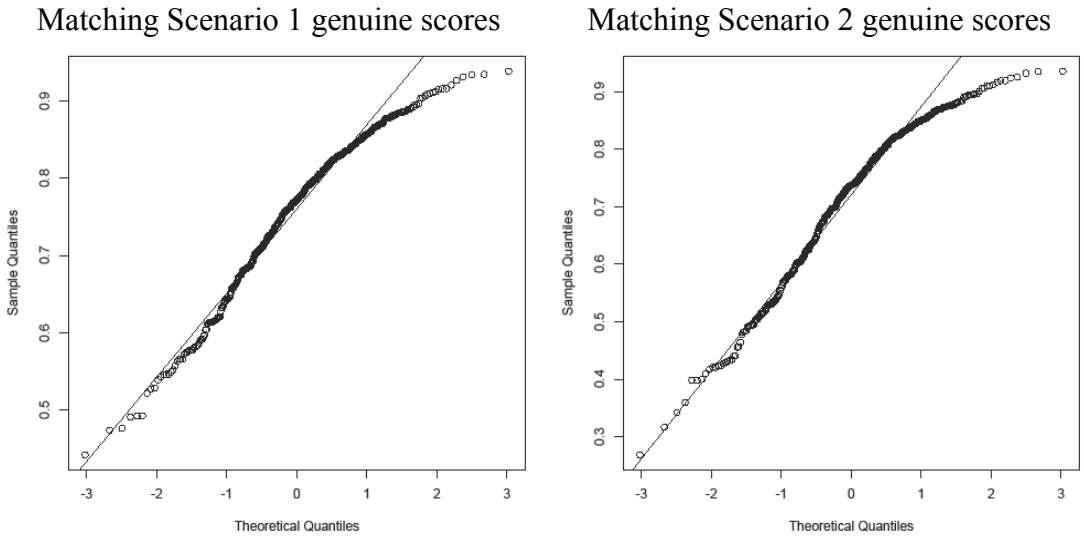

Figure 15. Normal Q-Q plots of the genuine matching scores for Matching Scenarios 1 and 2.

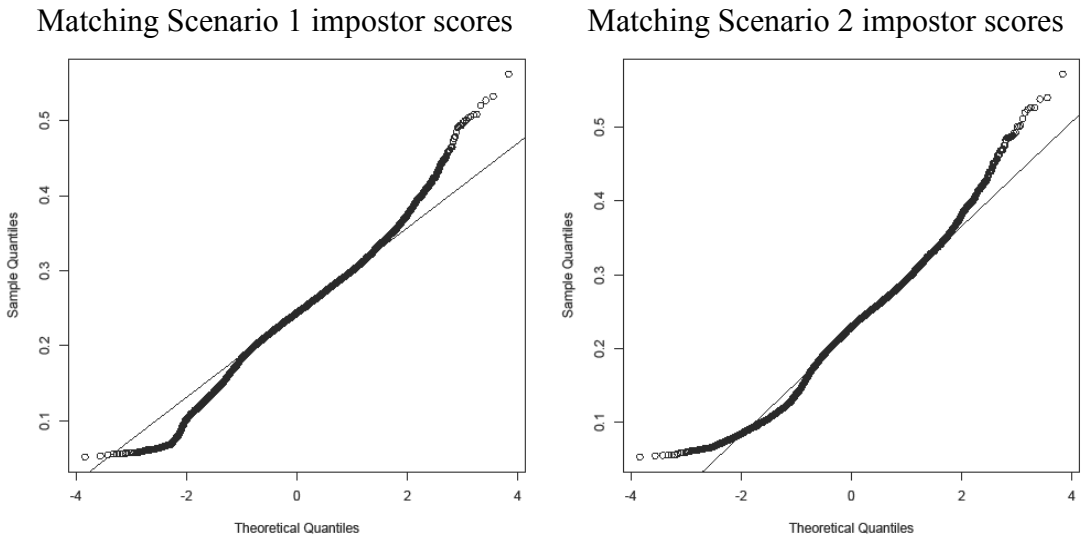

Figure 16. Normal Q-Q plots of the impostor matching scores for Matching Scenarios 1 and 2.

The density distributions for both board-to-cant matching scenarios are shown in Figure 17. They display the overlaps between the two distributions as well as the change in the distributions between the matching scenarios, indicating changes in matching scores over time. The figure shows that small portions of the genuine and impostor distributions overlap in both matching scenarios. In Matching Scenario 2, the variance between the matching scores increased while the mean matching scores decreased in the genuine and impostor distributions.

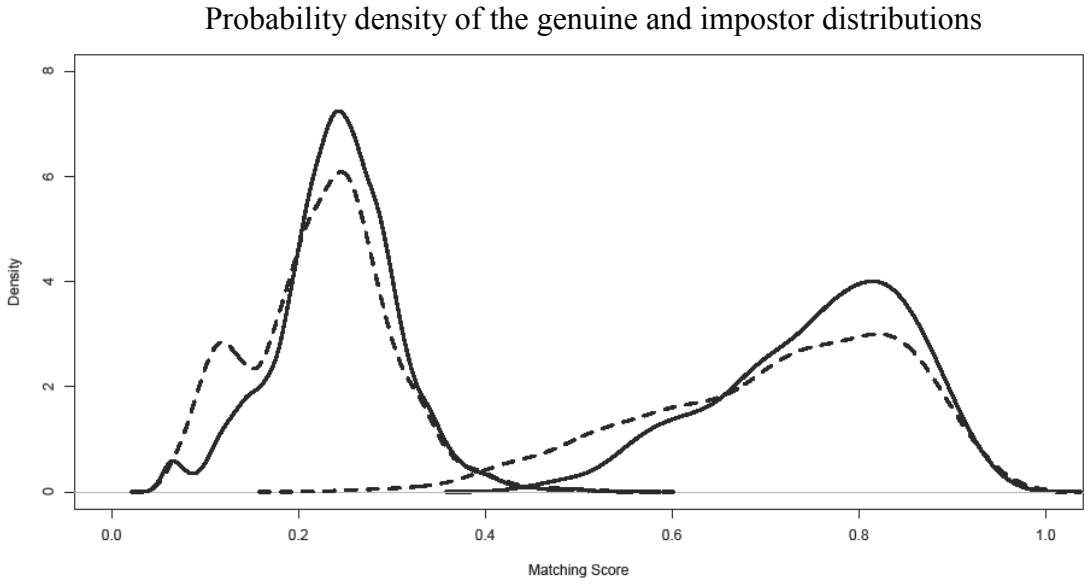

Figure 17. Density distributions of the genuine and impostor matching scores for Matching Scenarios 1 (solid line) and 2 (dotted line), showing overlapping distributions.

The board-to-cant ROC curves are shown in Figures 18 and 19. For Matching Scenario 1, there is only a slight curvature in the ROC's upper left-hand corner between the threshold values of 0.4 and 0.5 producing a curve with nearly

perpendicular lines (Figure 18). The Area Under the Curve (AUC) was 0.999959 indicating a very high probability that a randomly chosen genuine individual would produce a higher matching score than an impostor individual. The ROC curve for Matching Scenario 2 shows greater curvature than that for Matching Scenario 1 between threshold values of 0.3 and 0.5 producing a slightly smaller AUC of 0.99841 (Figure 19).

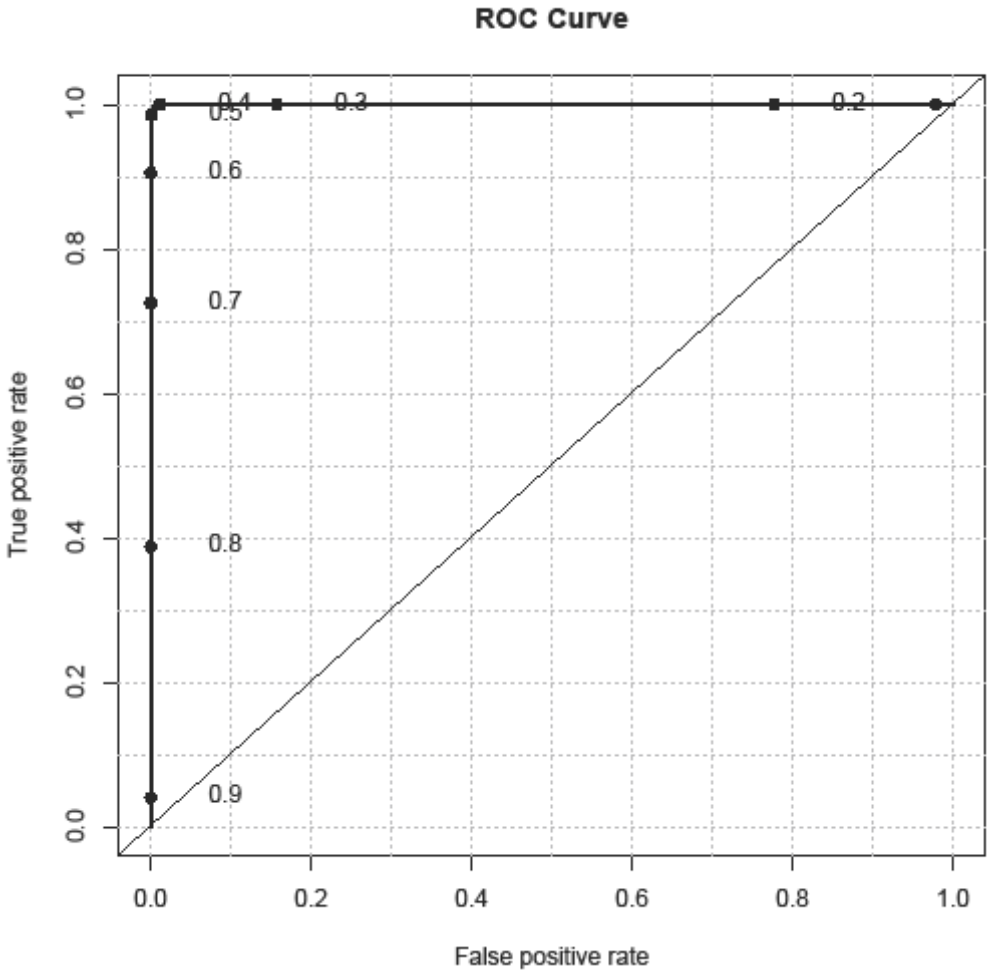

Figure 18. Receiver operating characteristic curve for Matching Scenario 1 with an AUC of 0.999959.

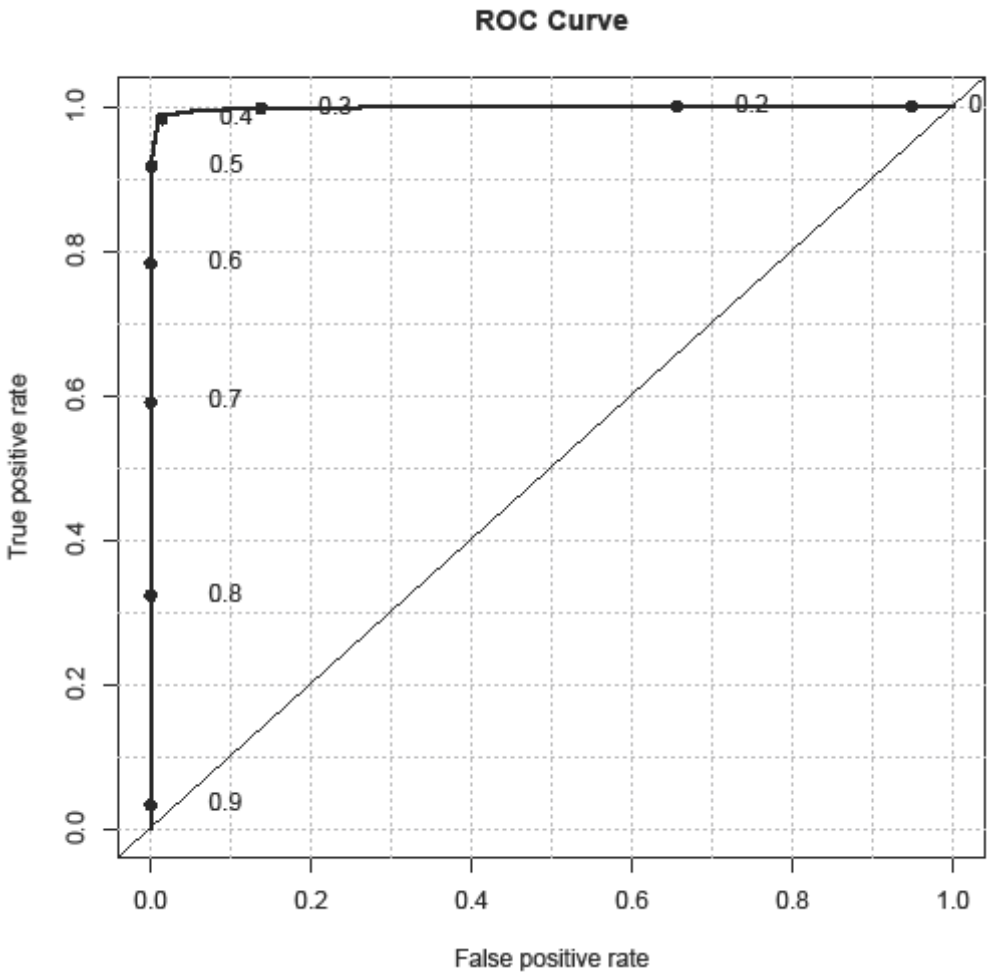

Figure 19. Receiver operating characteristic curve for Matching Scenario 2 with an AUC of 0.99841.

Table 9 presents the AUC along with the maximum accuracy (ACC) and its associated true positive rate (TPR) and threshold value for each Matching Scenario. The TPR is given to provide the algorithm's matching rate without the distortion of the overwhelmingly large impostor population. The results show a decrease in AUC, ACC, TPR, and threshold values between Matching Scenarios 1 and 2.

Table 9. AUC, maximum accuracy, true positive rate at the corresponding threshold value for the board-to-cant matching results.

	AUC	Max ACC	TPR at Max ACC	Threshold value
Matching Scenario 1 (Day 1 cants and Day 2 boards)	0.99959	0.99893	0.9850	0.5212
Matching Scenario 2 (Day 2 cants and Day 3 boards)	0.99841	0.99524	0.9275	0.4933

4.2. Cant-to-round matching results

The summary statistics for Matching Scenario 3 (Day 2 cants to Day 1 rounds) and Scenario 4 (Day 3 cants to Day 2 rounds) are shown in Table 10. For both matching scenarios, the genuine and impostor populations were statistically different from each other (Welch two sample t-test p-value < 0.0001). There was a slight, but insignificant, decrease in mean genuine matching scores between Matching Scenarios 3 and 4 (Welch two sample t-test p-value = 0.3221). There was also an insignificant increase in mean impostor matching scores (Welch two sample t-test p-value = 0.2344). The matching score variance for the genuine populations increased from scenario 3 and 4, but was insignificant (Fisher's f-test p-value = 0.1178), while the variance for the impostor populations showed a significant increased from Matching Scenarios 3 and 4 (Fisher's f-test p-value < 0.0001).

Table 10. Summary statistics describing the genuine and impostor matching scores for each cant-to-round matching scenario.

	Matching Scenario 3		Matching Scenario 4	
Distribution	Genuine n = 100	Impostor n = 2000	Genuine n = 100	Impostor n = 2000
Mean	0.7304	0.3458	0.7158	0.3495
Median	0.7509	0.3414	0.7342	0.3362
Variance	0.00918	0.00843	0.01259	0.01137
Range	[0.4357, 0.9604]	[0.0901, 0.6352]	[0.3966, 0.9351]	[0.0795, 0.6989]

Figure 20 shows the histogram distributions of the genuine matching scores for the cant-to-round matching scenarios. Tests showed that both Matching Scenario 3 and 4 could be considered to have normal distributions with slight negative skews. Figure 21 presents the histograms of the impostor matching scores, which show a generally normal distribution with a slight positive skew. Figures 22 and 23 display the normal QQ plots for the genuine and impostor scores for Matching Scenarios 3 and 4, and show slight deviations in normality.

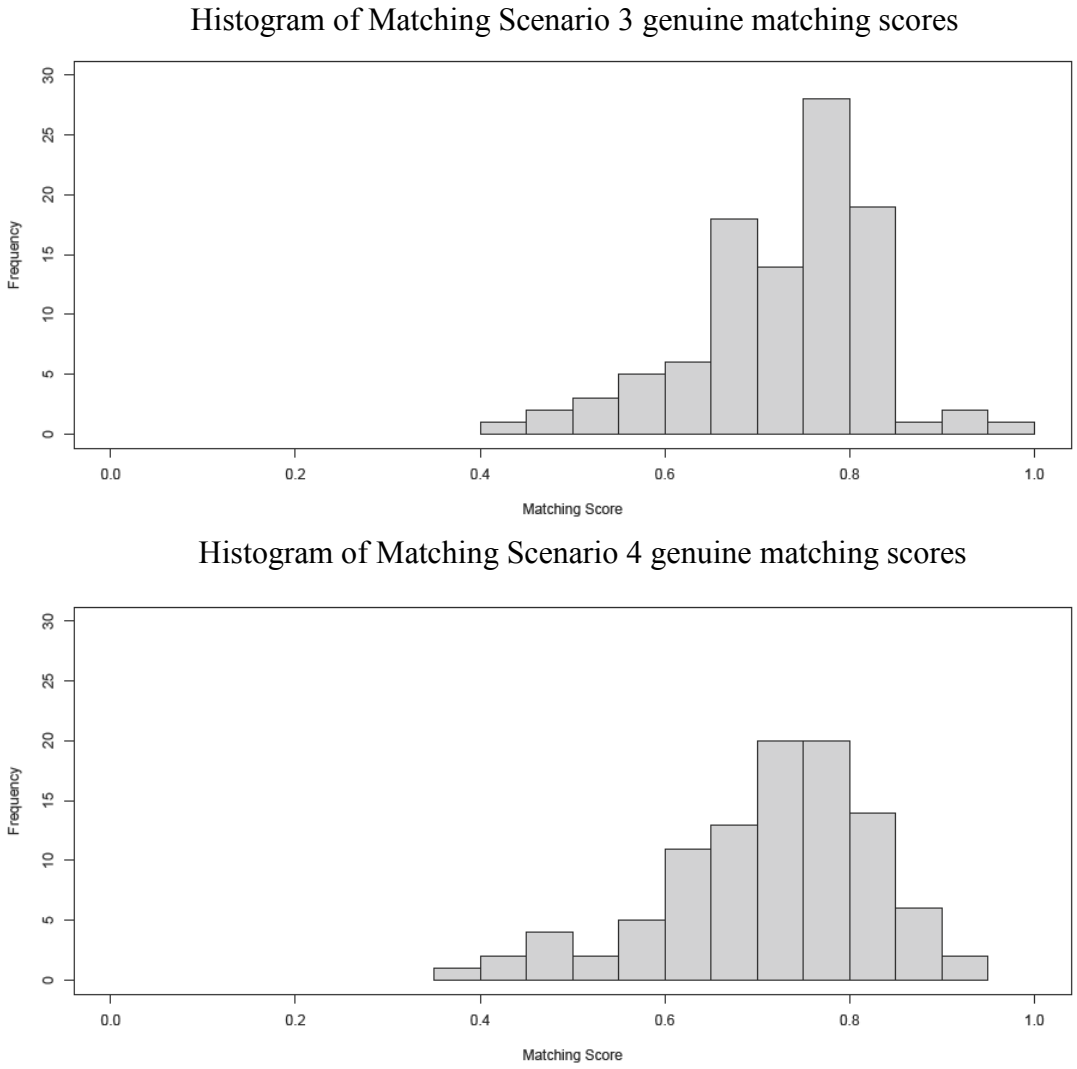

Figure 20. Histogram of the genuine matching scores for both cant-to-round matching scenarios, each showing negative skew (n = 100).

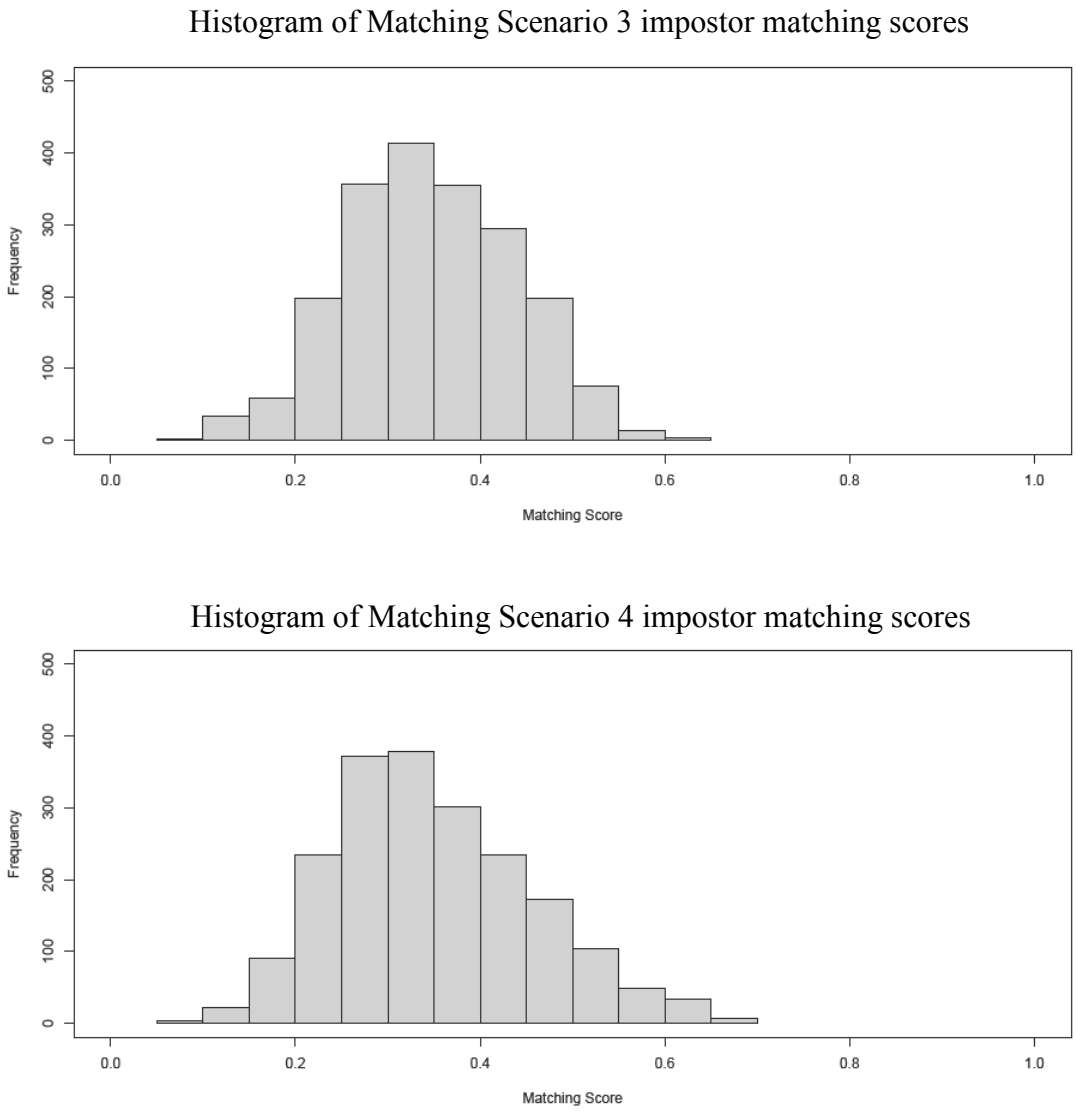

Figure 21. Histogram of the impostor matching scores for both cant-to-round matching scenarios, each showing positive skew (n = 2000).

Matching Scenario 3 genuine scores

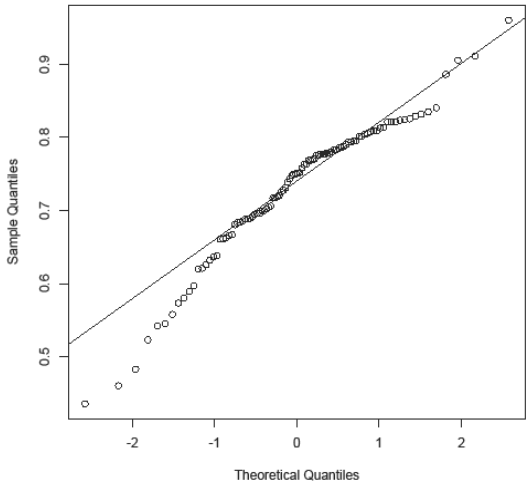

Matching Scenario 4 genuine scores

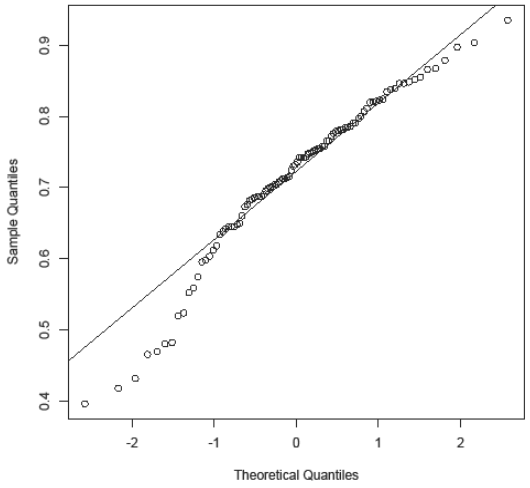

Figure 22. Normal Q-Q plots of the genuine matching scores for matching scenarios 3 and 4.

Matching Scenario 3 impostor scores

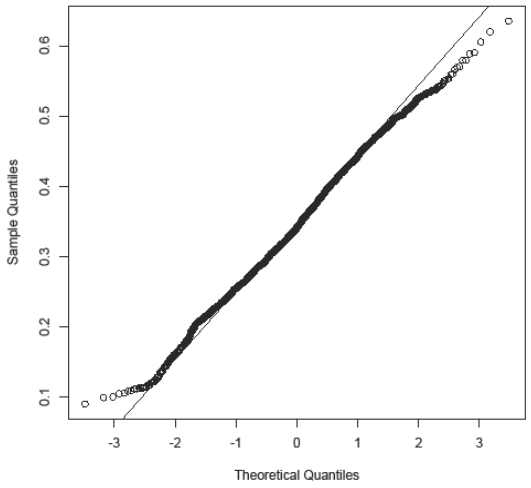

Matching Scenario 4 impostor scores

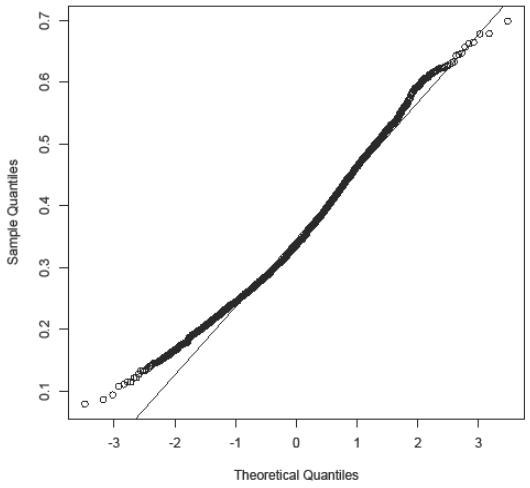

Figure 23. Normal Q-Q plots of the impostor matching scores for matching scenarios 3 and 4.

The density distributions for Matching Scenarios 3 and 4 are presented in Figure 24 and display an overlap between the genuine and impostor populations in both scenarios. These distributions have more overlap than the board-to-cant matching scenarios. When comparing Matching Scenarios 3 and 4, the variance between the matching scores increased while the mean matching scores decreased in the genuine distribution. The impostor distribution, however, did not significantly change between Matching Scenarios 3 and 4.

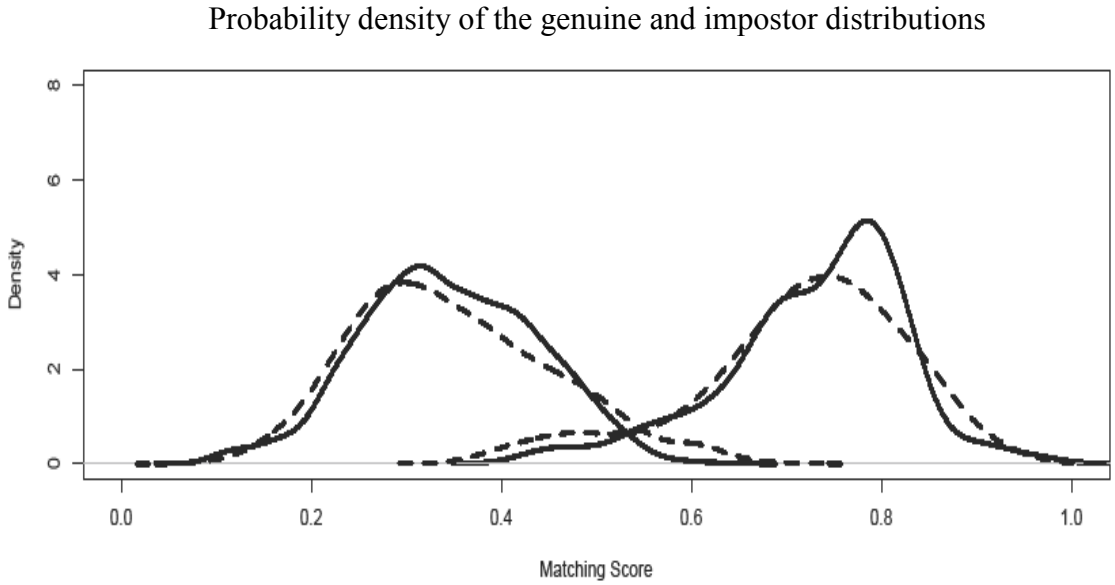

Figure 24. Density distributions of the genuine and impostor matching scores for Matching Scenarios 3 (solid line) and 4 (dotted line), showing overlapping distributions.

The ROC curves for Matching Scenario 3 and 4 are presented in Figures 25 and 26. In Matching Scenario 3, there is some curvature found between threshold

values of 0.4 and 0.6 (Figure 25), but there is more curvature in Matching Scenario 4 between threshold values of 0.4 to 0.65 (Figure 26). Table 11 presents the AUC along with the maximum accuracy (ACC) and its associated true positive rate (TPR) and threshold value for Matching Scenarios 3 and 4. The table shows a decrease in the AUC, ACC, and TPR between Matching Scenarios 3 and 4, while there is an increase in the threshold values between the two scenarios.

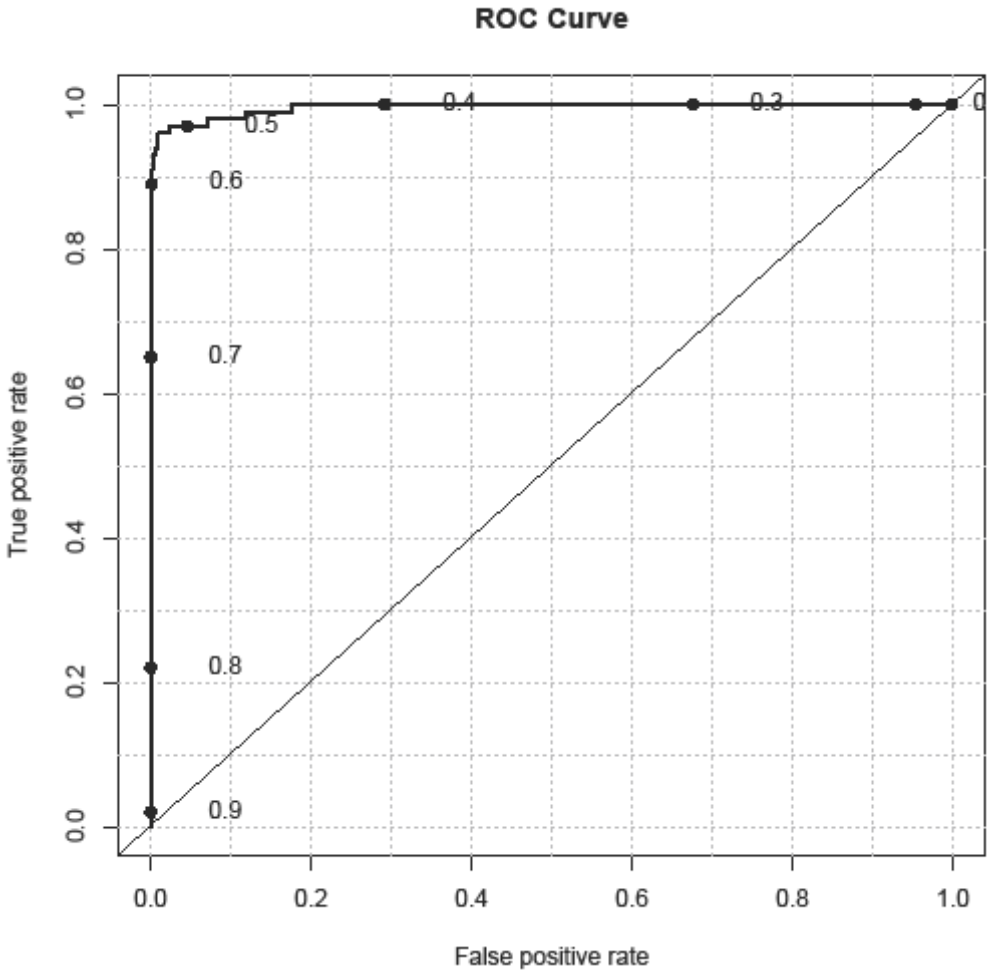

Figure 25. Receiver operating characteristic curve for Matching Scenario 3 with an AUC of 0.99574.

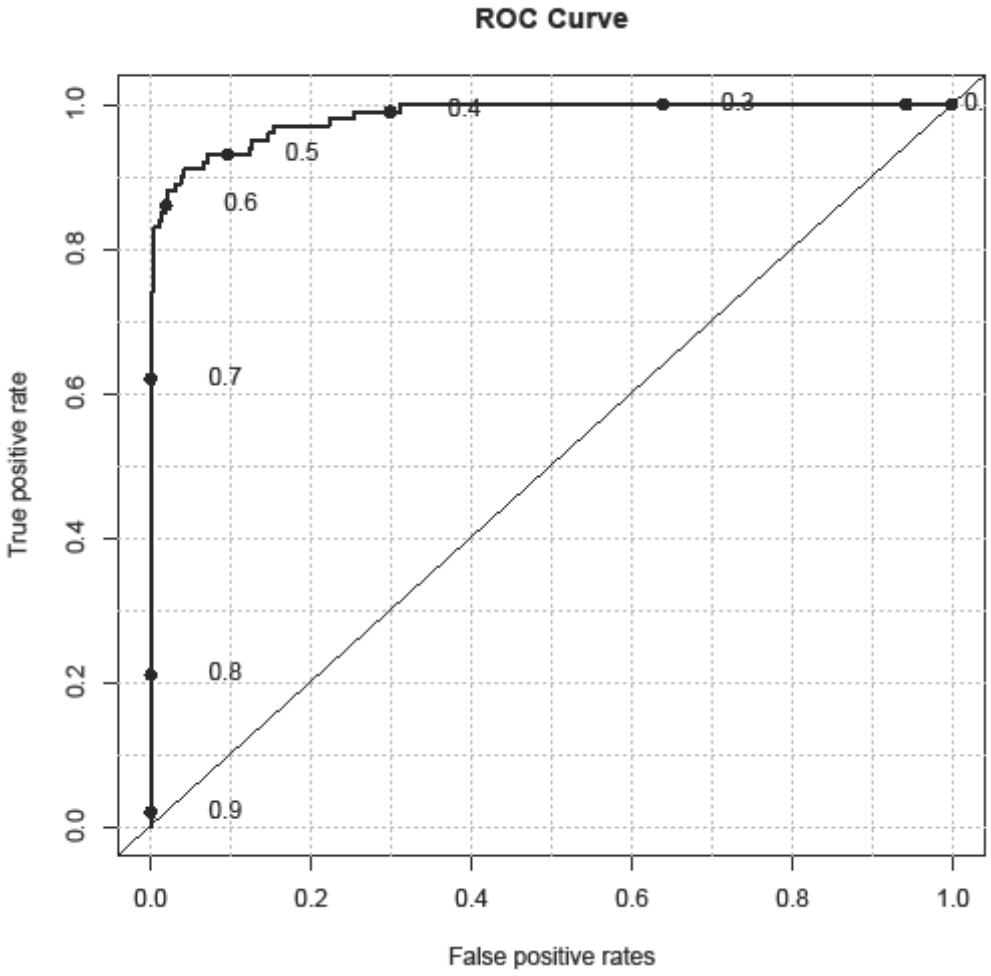

Figure 26. Receiver operating characteristic curve for Matching Scenario 4 with an AUC of 0.98292.

Table 11. AUC, maximum accuracy, true positive rate at the corresponding threshold value for the cant-to-round matching results.

	AUC	Max ACC	TPR at Max ACC	Threshold value
Matching Scenario 3 (Day 1 cants and Day 2 boards)	0.99574	0.99381	0.88	0.6209
Matching Scenario 4 (Day 2 cants and Day 3 boards)	0.98292	0.98762	0.83	0.6340

5. DISCUSSION

To establish if images of wood end-grain can theoretically be used for biometric identification, we will consider if the four requirements of universality, distinctiveness, permanence, and collectability are met. There appears to be three universal characteristics in end-grain with sufficient variability to provide the needed distinctiveness for biometric identification. Annual ring structure, heartwood shape, and surface texture were present in all our images and were probably the major factors responsible for image differentiation. Because our technique did not use any feature extraction, there is no way to determine which characteristic provided the most information. However, it seems intuitive that annual ring structure is the most variable characteristic, while surface texture is the least.

Knots and cracks were not present in all images and are, therefore, not universal characteristics. Only about 20% of the samples had knots present on the imaged surface, while about 10% had at least one surface crack. The presence of these non-universal characteristics undoubtedly affects the matching scores, but it could not be determined to what extent. However, it seems reasonable that any characteristic present in only a few individuals will assist in identification because it reduces the number of potential matches to images that possess the characteristic.

The fact that end-grain meets the distinctiveness requirement is evident from the high identification rates in Tables 9 and 11 and is demonstrated in the ROC curve graphs in Figures 18, 19, 25, and 26. The ACC values in these figures show identification rates in the nineties for board-to-cant matches and somewhat lower rates

in the eighties for cant-to-round matches. The small areas of overlap between the genuine and impostor matching score distributions shown in Figure 17 and 24 also visually demonstrate that there are significant differences among the end-grain of individuals at the board and cant levels. All of the matching results agree with the studies by Chiorescu et al. (2003), Chiorescu and Grönlund (2004a), and Charpentier and Choffel (2003) that found high rates of identification could be achieved using wood biometrics. In fact, matching rates could be improved by including a length filter or by matching both sides of a workpiece simultaneously.

The same evidence used to demonstrate distinctiveness also demonstrates that end-grain possesses permanence as well -- at least over the three-day time period of this study. The ROC curves for both the board-to-cant and the cant-to-round matching clearly showed that end-grain is distinctive. However, they also show that there was a slight deterioration in permanence as ninety-eight percent of the Day 2 boards were matched to their respective Day 1 cants, while only 93% were matched between Day 2 boards and Day 3 cants. These results indicate some deterioration in permanence, as was expected. Over 88% of the Day 2 cants were correctly matched back to their respective Day 1 rounds, decreasing to an 83% match between Day 2 and Day 3. These results were lower than the board-to-cant matching scenarios most likely because lower-resolution images were used to reduce computer-processing time.

We assume the deterioration in permanence is due to changes in end-grain because moisture content was not controlled in this study. However, the characteristics still remained fairly stable as shown by the matching score variances in

Figures 17 and 24, and by the maximum 4% change in the matching scores' mean values, which is statistically significant but practically insignificant.

While the length of time between the matching scenarios were the same, the results were lower when Day 2 and Day 3 images were matched for both board-to-cant and cant-to-round matching scenarios. This likely resulted from two factors: a change in annual ring dimensions and early/latewood contrast as the surface moisture content decreased with time. The images were taken over a span of three days and the samples remained exposed in a laboratory with lower equilibrium moisture content conditions. However, moisture content did not change enough to cause the samples to crack, but it did decrease enough to cause minimal shrinkage and slight changes in annual ring dimensions. The lower surface moisture content also reduced contrast, which decreased the differences between characteristics (Figure 27) such as the annual rings, surface texture, and heartwood making them more difficult to detect.

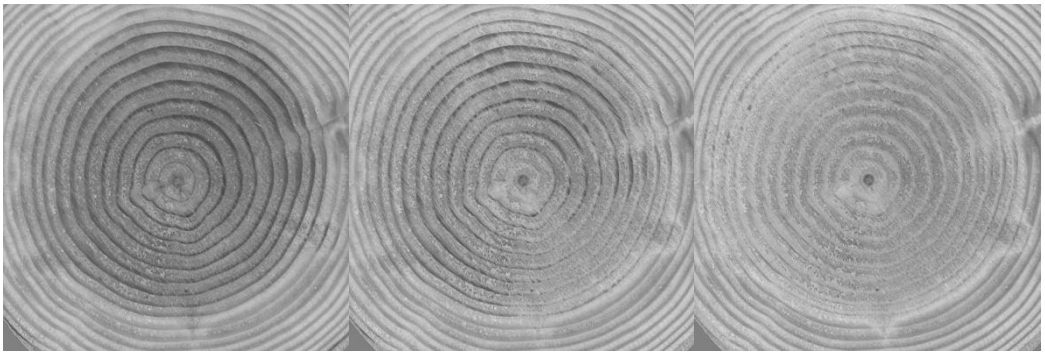

(a) Day 1 (b) Day 2 (c) Day 3

Figure 27. The visual changes in one cant's visual contrast from Day 1, Day 2, and Day 3.

End-grain characteristics were also shown to be collectable using digital imaging with sufficient resolution to maintain individual identities. This was true even after reducing the resolution by 50% in the board-to-cant matching scenarios and 75% in the cant-to-round matching scenarios. The original 24-bit color images were also converted to 8-bit grayscale to limit the amount of data handling, and despite the loss of the color information, the TPR was still 93% for the board-to-cant matching and 83% for cant-to-round matching when matching Day 2 images to Day 3 images.

Because the images have different pixel resolutions, we could not compare the board-to-cant and cant-to-round results directly. We can, however, infer that increasing pixel size reduces image detail and can lead to a reduction in image variability, which can reduce identification rates as reported by Chiorescu et al. (2003). The results seem to suggest that pixel resolution is more important than color information for imaging annual rings, which has been found in other studies (Brunner et al. 1990; Chiorescu et al. 2003).

The results of this study support the notion that end-grain characteristics are indeed usable for identification of boards to cants and cants to rounds, but there are some factors with the potential to affect the results that should be discussed. The origin of the logs used in this study is unknown, and it is likely that they came from different stands, which could increase end-grain variability because of different growing environments, or genetic stock. Trees from the same stand should tend to have more similar end-grain patterns.

The genuine and impostor matching score distributions showed signs of negative and positive skew, respectively. This is seen when comparing the genuine distributions with the impostor distributions; the genuine distributions exhibit generally more skew than the impostor distributions. This could be caused by the bounded matching score range, as confirmed by Mansfield and Wayman (2002), who state that biometric matching score distributions are likely to be skewed as they are located near the upper and lower ranges, especially when sample sizes are small. These deviations are generally acceptable, especially in a feasibility study such as ours.

Another explanation for this skewness is that a small number of impostor samples were simply more similar to some templates than others. Twins, or two different individuals that have very similar characteristics, were common in the Chiorescu et al. (2003) and Chiorescu and Grönlund (2004a) studies. It is unknown how unique end-grain characteristics are with regard to a larger population, but should be less of a problem in a sawmill where the number of logs in the system is limited at any one time.

The results between board-to-cant and cant-to-round matching scenarios could not be directly compared because they use images with pixels of two different sizes. The averaging of pixel values necessary to reduce image resolution may have removed useable information, or even introduced systematic noise, into the images, which could reduce the true positive rate.

Similarly, we cannot compare the results of this study to related studies using a similar methodology because the matching results represent single observations, and not known probability distributions (Mansfield and Wayman 2002; Fawcett 2006). Without matching score calibration, study results can be compared only when the individual studies use the same technique and matching algorithm (Fawcett 2006).

6. CONCLUSIONS AND FUTURE RESEARCH RECOMMENDATIONS

From this study's result, we conclude that end-grain meets the four requirements for biometric identification of universality, distinctiveness, permanence, and collectability and that a sawmill tracking system based on it is feasible. Therefore, end-grain should join the wood characteristics explored by Chiorescu et al. (2003), Chiorescu and Grönlund (2004a), Flodin et al. (2008), and Charpentier and Choffel (2003) that could potentially be used for biometric identification.

There are four areas that warrant further research. The effect of time on the permanence of end-grain characteristics should be explored further, even though a sawmill's short processing times should render it relatively unimportant to a real-world system. We would like to match the day 1 images to the day 3 images; something we were unable to explore due to time constraints. We expect the identification rates would be less than those between the day 2 and day 3 images as the end-grain experienced two full days of moisture loss between imaging.

The effect of pixel resolution warrants study in a more systematic manner because we matched the boards to cants using 100 pixel per inch (ppi) images, and the cants to rounds using 50 ppi images to reduce computer run times from months to weeks. Repeating this process using 100 ppi, 50 ppi, and 25 ppi images would indicate the importance of image detail on identification rates and provide information on which pixel resolution performs best. It would also allow us to directly compare

the board-to-cant and cant-to-round scenarios to determine the effect of sub-image area on identification results.

The effect of end-grain's surface roughness should also be explored because our samples had relatively smooth surfaces that may not represent the typical end-grain cut. A small sample study using cross-sections obtained from a sawmill log bucking station would test how smooth end-grain surfaces must be for identification.

Finally, the underlying question of whether annual ring structure alone can identify individuals should be explored. The question of how much annual rings contribute to identification rates is important because they are less likely to be altered during processing, whereas surface texture is more likely to be altered by impacts and moisture content changes. Extracting the annual rings also greatly reduces the data manipulated by the matching algorithm.

This study has shown end-grain can be an effective surface for identification between a sawmill's headrig and gangsaw. While there is a long way to go before an end-grain biometric identification system can be implemented in a sawmill, it is encouraging that this feasibility study has shown evidence that end-grain variability can lead to high identification rates.

7. BIBLIOGRAPHY

Brunner, C.C., G.B. Shaw, D.A. Butler, and J.W. Funck. 1990. Using color in machine vision systems for wood processing. Wood and Fiber Science. 22(4), pp. 413-428.

Charpentier, P., and D. Choffel. 2003. The feasibility of intrinsic signature identification for the traceability of pieces of wood. Forest Products Journal. 53(9), pp. 40-46.

Chiorescu, S., P. Berg, and A. Grönlund. 2003. The fingerprint approach: Using data generated by a 2-axis log scanner to accomplish traceability in the sawmill's log yard. Forest Products Journal. 53(2), pp. 78-86.

Chiorescu, S., and A. Grönlund. 2004a. The fingerprint approach: Using data generated by a 3D log scanner on debarked logs to accomplish traceability in the sawmill's log yard. Forest Products Journal. 54(12), pp. 269-276.

Chiorescu, S. and A. Grönlund. 2004b. The fingerprint Method: Using Over-bark and Under-bark Log Measurement Data Generated by Three-dimensional Log Scanners in Combination with Radiofrequency Identification Tags to Achieve Traceability in the Log Yard at the Sawmill. Scandinavian Journal of Forest Research. 19(4), pp. 374-383.

Chiorescu, S., and S. Grundberg. 2001. The influence of missing bark on measurements performed with a 3D log scanner. Forest Products Journal. 51(9), pp. 78-86.

Fawcett, T. 2006. An introduction to ROC analysis. Pattern Recognition Letters. 27(2006), pp. 861-874.

Flodin, J., J. Oja, and A. Grönlund. 2008. Fingerprint traceability of sawn products using industrial measurement systems for x-ray log scanning and sawn timber surface scanning. Forest Products Journal. 58(11), pp. 100-105.

Funck, J.W., Y. Zhong, D.A. Butler, C.C. Brunner, and J.B. Forrer. 2000. A Performance Analysis of Image Segmentation Algorithms As Applied to Wood Surface Feature Detection. Proceedings of Image Processing and Scanning of Wood. 2000. pp. 129-141.

Jain, A.K., A. Ross, and S. Prabhakar. 2004. An Introduction to Biometric Recogntion. IEEE Transactions on Circuits and Systems for Video Technology. 14(1), pp. 4-20.

Jain A. and S. Pankanti. 2001. Biometrics Systems: Anatomy of Performance. IEICIE Transactions Fundamentals. E00-A(1), pp. 1-11.

Kline, D.E., J.K. Wiedenbeck, P.A. Araman. 1992. Management of wood products manufacturing using simulation/animation. Forest Products Journal. 42(2), pp. 45-52.

Lu, B.H., R.J. Bateman, and K. Cheng. 2006. RFID enabled manufacturing: fundamentals, methodology, and applications. International Journal of Agile Systems and Management. 1(1), pp. 73-92.

Luis-Garcia, R., C. Alberola-Lopez, O. Aghzout, J. Ruiz-Alzola. 2003. Biometric identification systems. Signal Processing. 83(12), pp. 2539-2557.

Maness, T.C. 1993. Real-time quality control system for automated lumbermills. Forest Products Journal. 43(7/8), pp. 17-22.

Mansfield, A.J. and J.L. Wayman. 2002. Best Practices in Testing and Reporting Performance of Biometric Devices. Centre for Mathematics and Scientific Computing. National Physical Laboratory. Version 2.01.

Milota, M.R., C.D. West, and I.D. Hartley. 2005. Gate-to-gate life-cycle inventory of softwood lumber production. Wood and Fiber Science. 35(CORRIM Special Issue), pp. 47-57.

Panshin A.J., de Zeeuw, C. 1980. Textbook of Wood Technology. 4th Edition. McGraw Hill Book Co., New York.

R Development Core Team. 2009. R: A language and environment for statistical computing. Version 2.10.1. R Foundation for Statistical Computing, Vienna, Austria. ISBN 3-900051-07-0, URL http://www.R-project.org.

Sing, T., O. Sander, N. Beerenwinkel, and T. Lengauer. 2009. ROCR: Visualizing the performance of scoring classifiers. R package version 1.0-4. http://CRAN.R-project.org/package=ROCR

Sirkka, A. 2008. Modelling Traceability in the Forestry Wood Supply Chain. ICDE Workshops 2008. pp. 104-105.

Ozanne, L.K. and R.P. Vlosky. 1997. Willingness to pay for environmentally certified products: The consumer perspective. Forest Products Journal. 47(6), pp. 1-8.

Vlosky, R.P. and L.K. Ozanne. 1998. Environmental certification of wood products: The U.S. manufacturers perspective. Forest Products Journal. 48(9), pp. 21-26.

Wagner, F.G., C.E. Keegan, R.D. Fight, and S. Willits. 1998. Potential for small-diameter sawtimber utilization by the current sawmill industry in western North America. Forest Products Journal. 48(9), pp. 30-34.

Wall, B. 1995. Materials Tracking: the a la carte approach that avoids data indigestion. Industrial Management & Data Systems. 95(1), pp. 10-11.

Wiedenbeck, J., and D.E. Kline. 1994. System simulation modeling: A case study illustration of the model development life cycle. Wood and Fiber Science 26(2), pp. 192-204.

Young, T.M., and P.M. Winistorfer. 1999. Statistical Process Control and the Forest Products Industry. Forest Products Journal. 49(3), pp. 10-17.